

13. SITE 725¹

Shipboard Scientific Party²

HOLE 725A

Date occupied: 22 September 1987
Date departed: 22 September 1987
Time on hole: 4 hr, 30 min
Position: 18°29.200'N, 57°42.030'E
Water depth (sea level; corrected m, echo-sounding): 311.5
Water depth (rig floor; corrected m, echo-sounding): 322.0
Bottom felt (m, drill pipe): 323.1
Penetration (m): 4.5
Number of cores: 1
Total length of cored section (m): 4.5
Total core recovered (m): 4.5
Core recovery (%): 100%
Oldest sediment cored
Depth sub-bottom (m): 4.5
Nature: nannofossil foraminifer sandy silt

HOLE 725B

Date occupied: 22 September 1987
Date departed: 22 September 1987
Time on hole: 8 hr, 15 min
Position: 18°29.200'N, 57°42.030'E
Water depth (sea level; corrected m, echo-sounding): 311.5
Water depth (rig floor; corrected m, echo-sounding): 322.0
Bottom felt (m, drill pipe): 323.1
Penetration (m): 93.8
Number of cores: 10
Total length of cored section (m): 93.8
Total core recovered (m): 11.2
Core recovery (%): 11.9
Oldest sediment cored
Depth sub-bottom (m): 93.8
Nature: foraminifer-rich calcitic sandy silt
Age: Pleistocene
Measured velocity (km/s): 1.6

HOLE 725C

Date occupied: 22 September 1987
Date departed: 22 September 1987
Time on hole: 9 hr, 45 min

Position: 18°29.200'N, 57°42.030'E
Water depth (sea level; corrected m, echo-sounding): 311.5
Water depth (rig floor; corrected m, echo-sounding): 322.0
Bottom felt (m, drill pipe): 322.7
Penetration (m): 162.8
Number of cores: 17
Total length of cored section (m): 162.8
Total core recovered (m): 98.8
Core recovery (%): 60.6
Oldest sediment cored
Depth sub-bottom (m): 162.8
Nature: nannofossil-rich calcitic sand, silt, and clay
Age: Pleistocene
Measured velocity (km/s): 1.6

Principal results: Site 725 is the shallow landward end point of a depth transect on the Oman continental margin. Our intention at Site 725 was to trace the fluctuations in the upper boundary of the oxygen-minimum zone through time and to evaluate these fluctuations with regard to changes in the monsoon, in tectonic evolution of the margin, and in sea level.
Findings at Site 725 include:

1. Organic- and opal-rich clayey silt alternates with nonlaminated nannofossil ooze and calcitic silty clay. Laminated intervals are confined to the upper part of the lower Pleistocene (lithologic Unit II) and are missing in both the lower (lithologic Unit III) and upper (lithologic Unit I) parts of the section.
2. The sedimentation rate averages about 120 m/m.y. over the top 120 m.
3. Opal occurrences are confined to laminated intervals and sediments having high organic-carbon concentrations of lithologic Units II and III.
4. Cold-water nannoplankton occurrences in the deepest part of the cored section.
5. Persistent occurrence of interstitial sulfate, high alkalinity, and dramatic core expansion suggest replenishment of the interstitial sulfate pool from a deep source comparable to that of Site 723.
6. Elevated ethane and propane gas concentrations with depth imply migration of thermogenic hydrocarbons from deep sources.

Site 725 constitutes a section of Pleistocene age that shows pronounced changes in the depositional environment, which are tentatively attributed to extension and intensification of the mid-water oxygen-minimum zone in the early Pleistocene. These changes were observed at other margin sites and are probably contemporaneous and of a regional rather than local extent.

BACKGROUND AND OBJECTIVES

Site 725 is located at 18°29.200'N and 57°42.030'E on the continental margin of Oman in a water depth of 311 m near the landward edge of the upper slope basin. The location of Site 725 is shown in Figures 1 and 2, and its structural and depositional setting is shown in Figure 3. Site 725 is located in the transitional zone between the continental shelf and the slope basin. The site lies near a faulted block that is thought to be part of an ophiolitic basement and that forms the eastern boundary of the slope basin. Seismic reflection profiles show eastward-dipping layers that both onlap and drape the underlying base-

¹ Prell, W. L., Niitsuma, N., et al., 1989. *Proc. ODP, Init. Repts.*, 117: College Station, TX (Ocean Drilling Program).

² Shipboard Scientific Party is as given in List of Participants preceding the contents.

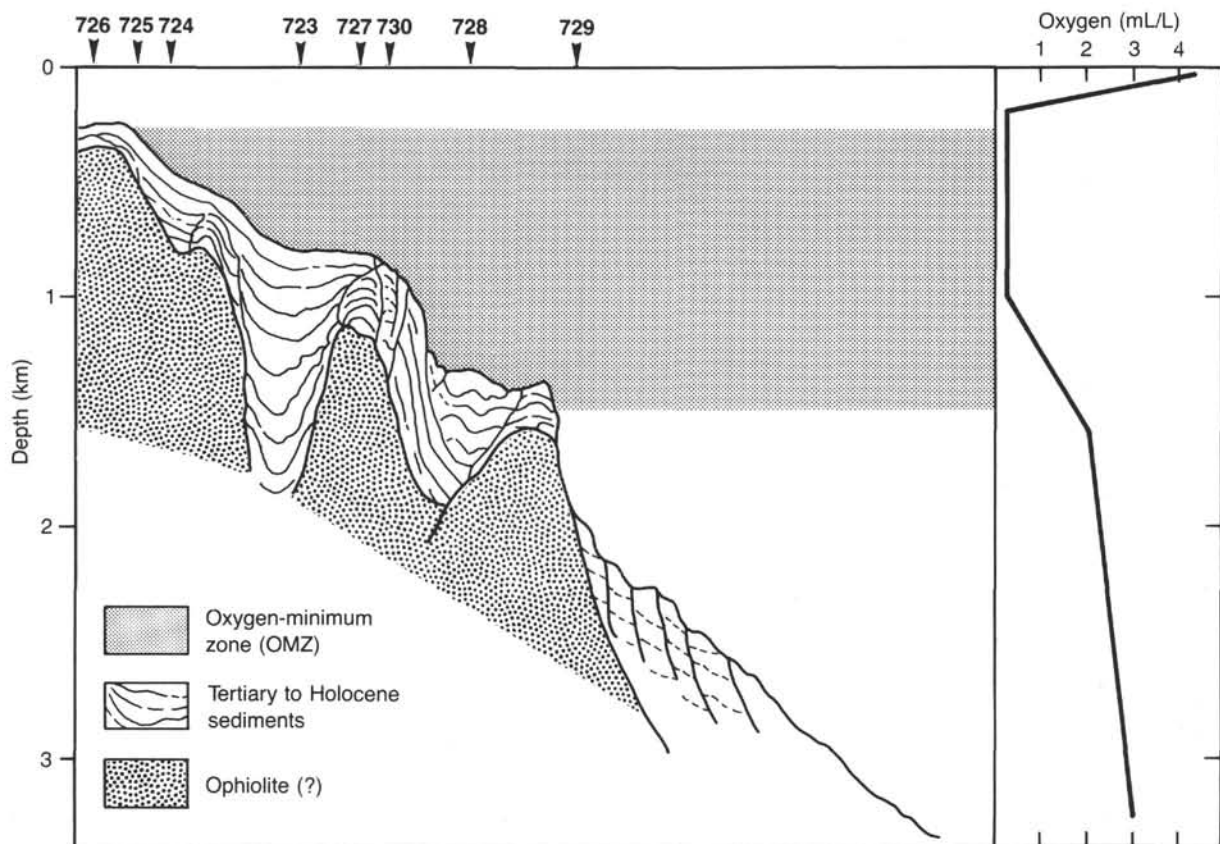


Figure 1. Structure of the Oman margin and the oxygen-minimum zone. The schematic drawing of the Oman margin shows the series of basement ophiolite blocks and the sedimentary basins between them. The concentration of oxygen in the water column (RC2704, unpubl. data) defines the depth range of the oxygen-minimum zone and where it impinges on the margin. The schematic location of Site 725 is indicated.

ment structures. Although the reflectors are generally conformable, some faulting and erosion is indicated by offset and converging reflectors. Site 725 was situated upslope of the original site location to avoid some of the subsurface structure. Preliminary correlation of seismic reflectors within the basin indicated that average accumulation rates should be high at Site 725, although winnowing of shelf-edge sediments might be possible. Site 725 was selected to provide the shallow end-member for a depth transect that spans the depth of the oxygen-minimum zone. The site was expected to provide a high-resolution sedimentary record of the variations of monsoonal upwelling and of the oxygen-minimum zone during the Pliocene-Pleistocene.

Specific objectives for drilling at Site 725 were:

1. To obtain a high-resolution record of the sediments associated with the near-coastal zone of the monsoonal upwelling system so as to establish changes in timing and intensity of the monsoon.
2. To provide the shallow end-member for a depth transect of sediments that will be used to examine the organic-rich sedimentary facies of the margin and to establish their relationship to the oxygen-minimum zone and its spatial variation through time.
3. To document the diagenetic processes associated with the oxygen-minimum zone and organic-rich sediments.
4. To search for evidence of changes in the structure of the intermediate water masses of the Arabian Sea during the Pliocene-Pleistocene.

OPERATIONS

The *JOIDES Resolution* arrived at Site 725 in a dynamic positioning mode by 0230 hr on 22 September 1987. This site, which previously had been surveyed jointly with Site 724, is located in a water depth of 311 m at 18°29.200'N and 57°42.030'E (see Fig. 4, "Operations" section, Site 724 chapter). Upon arrival, a shallow-water beacon was lowered on a taut wire, and by 0430 hr Core 117-725A-1H had been shot. The core barrel parted while shooting Core 117-725A-2H, and Hole 725A had to be abandoned. Recovery of Core 117-725A-1H (0–4.5 meters below seafloor [mbsf]) was 100% (Table 1).

Without offset, Hole 725B was spudded at 0600 hr on September 22 in extended-core-barrel (XCB) coring mode. Ten XCB cores recovered only 11.9% of the cored interval, which was dominated by sand and silt from 0 to 93.8 mbsf. After Core 117-725B-10X had been retrieved, coring in Hole 725B was suspended and the drill string pulled. Hole 725C was spudded at 1415 hr on 22 September, 20 m northeast of Hole 725B, after bit modification.

Three advanced piston corer (APC) cores recovered 100% of the interval from 0 to 28.5 mbsf until an overpull of 80,000 lb made XCB coring necessary. Cores 117-725C-4X through -17X (28.5–162.8 mbsf) showed a much improved recovery, after bit modification, of 52.3% in Hole 725C. Overall recovery in Hole 725C was 60.6%. After reaching total depth, the hole was displaced with weighted mud. After clearing the mud line and retrieving the beacon, the ship was under way to Site 726 by 2400 hr on 22 September 1987.

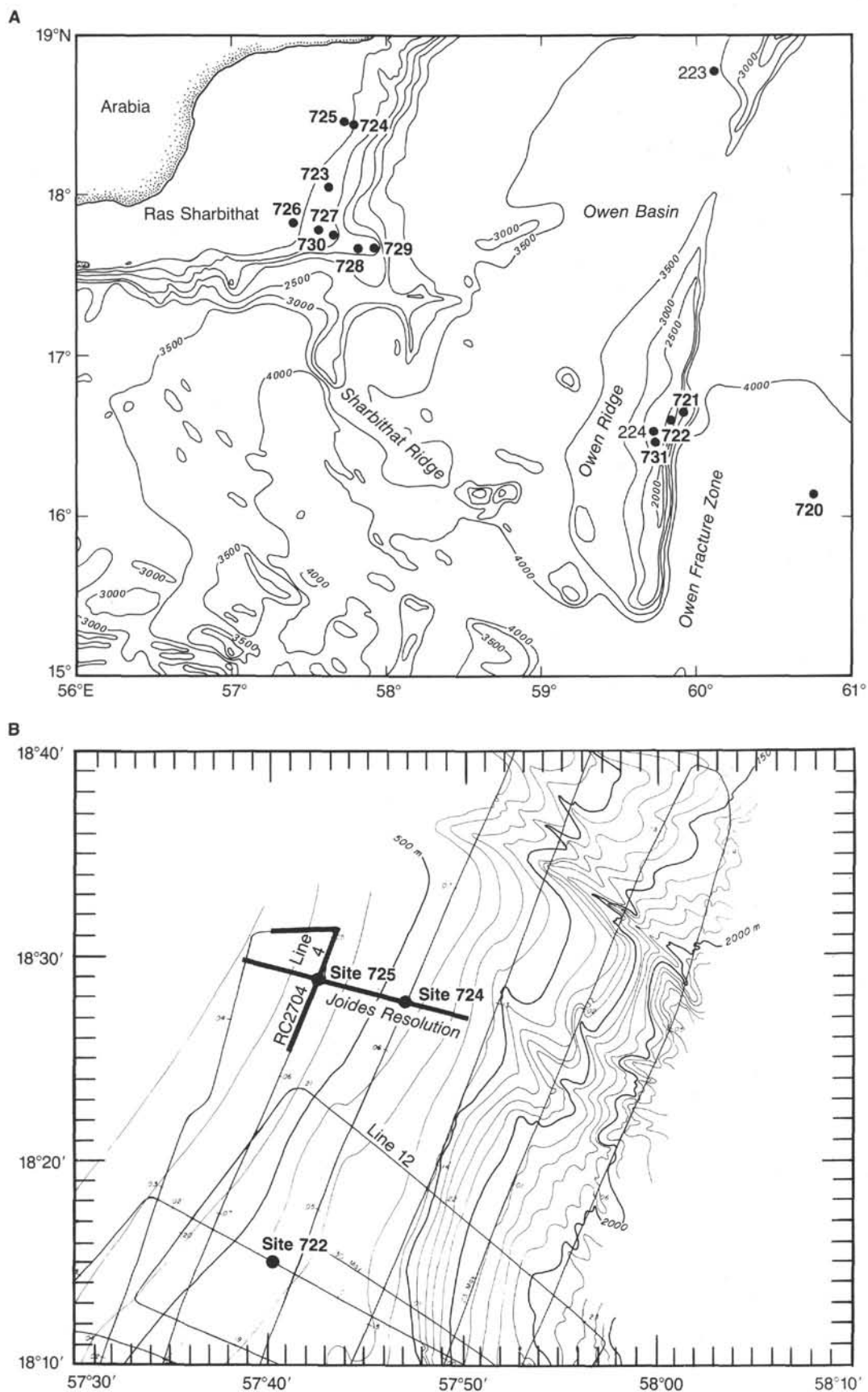


Figure 2. **A.** Bathymetry of the Oman margin and the location of Site 725. **B.** The detailed location of Site 725 and the seismic profiles shown in Figure 3. Bathymetry and seismic data are from the site survey (RC2704, 1986).

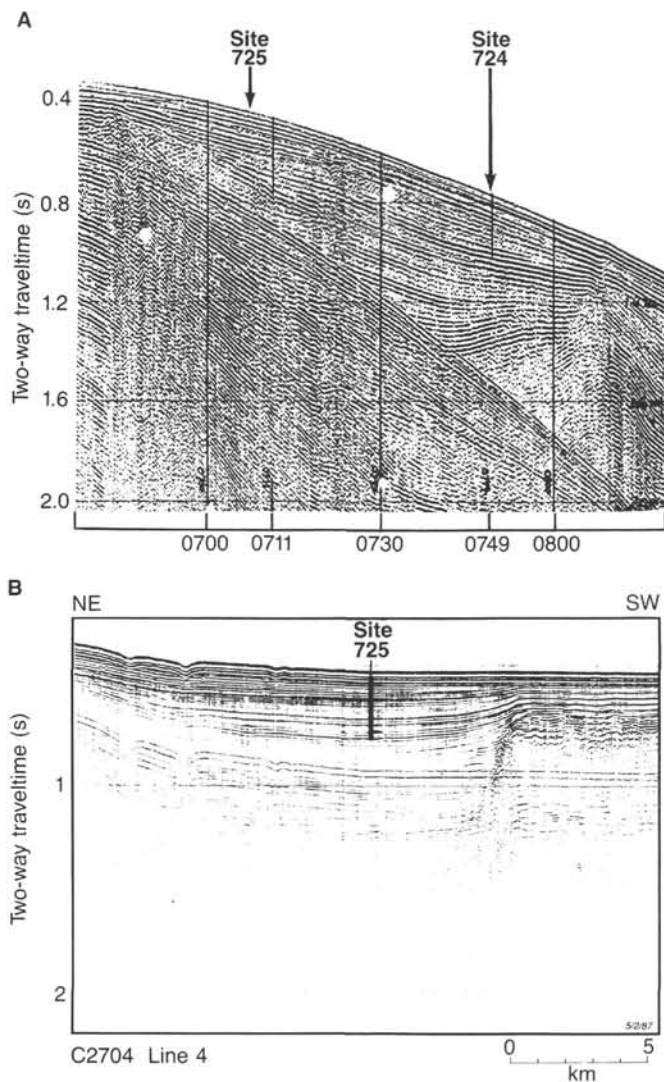


Figure 3. **A.** Single channel seismic (SCS) reflection profiles showing the structural and depositional setting of Site 725. Line 4 of *JOIDES Resolution* is perpendicular to the trend of the basin and shows the bounding basement blocks and the synclinal-shaped sediment fill. **B.** RC2704 Line 4 is along the strike of the basin and shows the thick sediments.

LITHOSTRATIGRAPHY

Lithologic Units

Site 725 is located on the shelf/slope transition of the Oman margin. The recovered sedimentary sequence ranges from Pleistocene to Holocene in age. Coring of Hole 725A was terminated after the first core because of core barrel failure. Because of poor recovery at Hole 725B, lithologic description and interpretation are based predominantly on sediments recovered from Hole 725C.

Sediments recovered at Site 725 are dominated by calcitic marly, nannofossil ooze, but also include calcitic marly calcareous ooze; interbedded clayey silt and laminated diatomaceous mud; and calcitic sand, silt, or clay. Detrital calcite is common to abundant in all these lithologies and may be derived from either an inorganic or a reworked biogenic source. The lithologic section has been divided into three units using visual core descriptions, compositional analyses of smear slides, and carbonate and organic carbon contents as distinguishing parameters. Lithologic Units I and III are compositionally similar; both are

dominated by biogenic calcareous components and characterized by bioturbation. Lithologic Unit II contains laminated diatomaceous deposits with interbedded detrital intervals. These sediments contain less inorganic calcite and biogenic carbonate than those in lithologic Unit I. The characteristics and occurrences of these units are summarized in Table 2 and Figure 4.

Unit I (Depth: Hole 725A, 0–4.5 mbsf; Hole 725B, 0–93.8 mbsf; Hole 725C, 0–120.0 mbsf; Age: Pleistocene to Holocene)

Cores 117-725A-1H, 117-725B-1X through 117-725B-10X, and 117-725C-1H through 117-725C-13X.

The composition of lithologic Unit I changes slightly downcore, from calcitic marly calcareous ooze and marly foraminifer nannofossil ooze near the surface to calcitic, marly nannofossil ooze and nannofossil-rich calcitic silty clay at its base. Colors in this unit gradationally darken downcore, from olive (5Y 4/3) and olive gray (5Y 4/2) near the surface, to olive (5Y 4/3), olive gray (5Y 4/2), and dark greenish gray (10Y 5/2) at intermediate levels, to olive (5Y 4/3), olive gray (5Y 4/2), dark olive gray (5Y 4/1 and 5Y 3/2), and very dark gray (5Y 3/1) lower in the section.

Unit I is slightly to moderately bioturbated except in Core 117-725C-11X, where faint laminations are locally developed.

From smear-slide analyses, lithologic Unit I contains 15% to 55% inorganic calcite, 5% to 20% quartz, 10% to 45% clays, 5% to 50% nannofossils, and 2% to 20% foraminifers (including abundant benthics; see “Biostratigraphy” section, this chapter). Feldspars, mica, dolomite, and accessory minerals are present in abundances of 1% to 5%, while phosphate concretions are locally present and glauconite occurs sparsely throughout. Volcanic glass is notably absent in Unit I, and biogenic siliceous components are present only in trace abundances at the base of the unit (Core 117-725C-13X). These compositional ranges indicate that terrigenous material is generally more abundant than biogenic constituents in Unit I and that the terrigenous components become more dominant downcore. In addition, clay content increases and the abundance of silt-size quartz decreases downcore in Unit I, suggesting that Unit I generally becomes more fine-grained downsection.

Unit II (Depth: 120.0–145.4 mbsf; Age: Pleistocene)

Cores 117-725C-13X through 117-725C-16X.

Lithologic Unit II is composed of interbedded calcitic sand-silt-clay, olive gray (5Y 4/2), and laminated diatomaceous beds. These laminated beds contain diatomaceous calcareous clayey silt; diatomaceous calcitic marly nannofossil ooze (olive [5Y 4/3], olive gray [5Y 4/2], and dark olive gray [5Y 3/2]); diatomaceous clayey silt (dark olive gray [5Y 3/2]); and diatomaceous mud (olive [5Y 5/3]). Smear-slide analyses indicate that the darker diatomaceous laminae contain 10% to 30% diatoms, 2% to 5% sponge spicules, 10% to 35% nannofossils, 1% to 5% foraminifers, 25% to 35% clays, 15% to 25% inorganic calcite, and 3% to 20% quartz. The light-colored, diatomaceous laminations have significantly different compositions, however, and average 55% diatoms, 30% clay, 3% inorganic calcite, and 2% to 5% each of quartz, nannofossils, and foraminifers. The calcitic sand-silt-clay intervals are essentially barren of biogenic components and contain 20% to 50% inorganic calcite, 10% to 45% clay, 20% to 30% quartz, and 0% to 5% siliceous biogenic material.

The character of the laminations within the diatomaceous intervals changes in Unit II from more diffuse laminations on a scale of 1 cm in Core 117-725C-14X (129–133 mbsf) to very well-defined, millimeter-scale lamination in Core 117-725C-15X (136–140 mbsf). Often, diatom assemblages within the lighter-colored diatomaceous laminae are nearly monospecific. The contact between the uppermost laminated zone and the overlying

Table 1. Coring summary at Site 725.

Core no.	Date (Sept. 1987)	Time	Depth (mbsf)	Cored (m)	Recovered (m)	Recovery (%)
117-725A-1H	22	0540	0-4.5	4.5	4.53	100.0
117-725B-1X	22	0700	0-7.5	7.5	0.22	2.9
2X	22	0750	7.5-17.1	9.6	0.36	3.8
3X	22	0910	17.1-26.6	9.5	0.62	6.5
4X	22	1015	26.6-36.2	9.6	2.95	30.7
5X	22	1050	36.2-45.7	9.5	2.35	24.7
6X	22	1130	45.7-55.3	9.6	1.03	10.7
7X	22	1205	55.3-64.9	9.6	2.08	21.6
8X	22	1235	64.9-74.5	9.6	0.06	0.6
9X	22	1255	74.5-84.1	9.6	0.78	8.1
10X	22	1320	84.1-93.8	9.7	0.77	7.9
117-725C-1H	22	1445	0-9.0	9.0	9.00	100.0
2H	22	1515	9.0-18.6	9.6	9.66	100.0
3H	22	1540	18.6-28.5	9.9	9.91	100.0
4X	22	1620	28.5-38.0	9.5	4.01	42.2
5X	22	1650	38.0-47.5	9.5	1.00	10.5
6X	22	1715	47.5-57.0	9.5	5.94	62.5
7X	22	1740	57.0-66.5	9.5	0.49	5.2
8X	22	1805	66.5-76.1	9.6	4.18	43.5
9X	22	1825	76.1-85.7	9.6	6.27	65.3
10X	22	1850	85.7-95.3	9.6	0.05	0.5
11X	22	1945	95.3-104.9	9.6	7.06	73.5
12X	22	1935	104.9-114.5	9.6	6.41	66.8
13X	22	1955	114.5-124.1	9.6	3.92	40.8
14X	22	2015	124.1-133.8	9.7	9.66	99.6
15X	22	2030	133.8-143.5	9.7	7.73	79.7
16X	22	2055	143.5-153.2	9.7	3.71	38.2
17X	22	2115	153.2-162.8	9.6	9.76	101.0

Table 2. Lithologic summary at Site 725.

Unit	Description	Facies	Depth (mbsf)	Core	Hole
I	Foraminifer calcitic sandy silts to calcitic marly calcareous ooze and calcitic marly nannofossil ooze to nannofossil-rich sand-silt-clay.	Hemipelagic and calcitic detrital facies	0-4.5	1H	A
			0-93.8	1X to 10X	B
			0-120.0	1H to 13X	C
II	Interbedded and laminated diatomaceous clayey silt, diatomaceous mud, and calcitic marly nannofossil ooze, calcitic sand silt clay.	Laminated and detrital facies	120.0-145.4	13H to 16H	C
III	Nannofossil-rich calcitic sand-silt-clay to calcitic marly nannofossil ooze	Hemipelagic and calcitic detrital facies	145.4-162.8	16X to 17X	C

ing unlaminated diatomaceous deposits of Unit II is sharp and lies beneath a basal foraminiferal sand.

Unit III (Depth: 145.4-162.8; Age: Pleistocene)

Cores 117-725C-16X to 117-725C-17X.

Lithologic Unit III is similar to lithologic Unit I in composition and appearance. It is dominated by calcitic marly nannofossil ooze, interbedded with olive (5Y 4/3), olive gray (5Y 4/2), and dark olive gray (5Y 3/2) intervals. Nannofossil-rich calcitic sand-silt-clay is present as a minor lithology, in olive gray (5Y 4/2) and dark olive gray (5Y 3/2) intervals 20 to 75 cm thick. Foraminifers and dispersed shell debris are common in Unit III, and the entire unit is slightly bioturbated.

The marly nannofossil oozes contain 25% to 45% nannofossils, 25% to 35% inorganic calcite, 20% to 25% clay, 5% to 11% quartz, and 2% to 5% each of foraminifers and accessory minerals. The sand-silt-clay intervals contain an average of 25% quartz, 25% clay, 35% inorganic calcite, 10% biogenic carbonate, and 5% accessory minerals.

Discussion

The sedimentary sequence at Site 725 was recovered from a shallow water depth on the Oman margin. For this reason, the depositional record preserved at Site 725 will provide valuable comparisons to correlative deposits from deeper-water environments elsewhere on the margin. The subdivision of the sequence at Site 725 into three lithologic units emphasizes variations in terrigenous and biogenic sediment abundances, as well as differences in depositional and preservational style (i.e., laminated vs. bioturbated intervals). The variations in abundances of sedimentary components are probably related to fluctuating rates of terrigenous sediment supply and marine planktonic productivity, which may have varied in response to climatic fluctuations during the Pleistocene.

At the base of Hole 725C, the bioturbated nannofossil-rich calcitic sand-silt-clays and calcitic marly nannofossil oozes of Unit III contain an important signature of marine planktonic influx (i.e., foraminifers, coccolithophores, and marine organic carbon). Despite the relatively high abundances of terrigenous components (generally greater than 50%), organic carbon con-

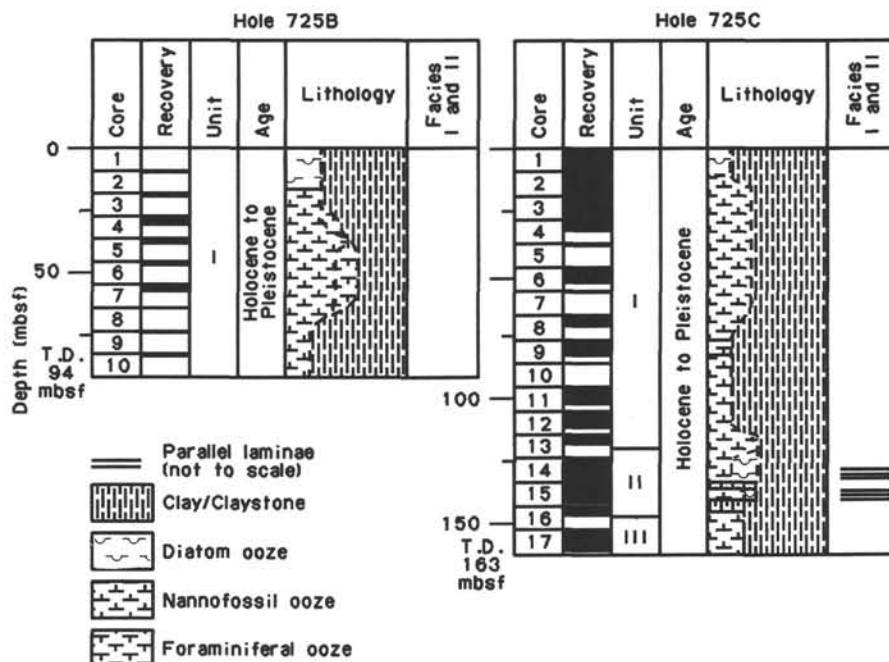


Figure 4. Lithologic summary, Site 725. Lithology is inferred between recovered intervals. Note: No lithologic summary for 725A (recovered only 1 core).

tents near 3% (Table 3 and Fig. 5) are characteristic of lithologic Unit III. The elevated level of organic carbon in lithologic Unit III can be attributed to either an increase in supply, which is related to primary productivity in surface water, or enhanced preservation. Changes in the amount of organic carbon preserved in marine sediments have been attributed to variations in sedimentation rate, bottom-water oxygen contents, and redox potential in the near-surface sediment (see Emerson, 1985, and references therein). Any of these could be factors at Site 725.

A significant contribution of biogenic silica at Site 725 is first evident in lithologic Unit II, which contains diatomaceous laminated intervals. The light layers in these laminated zones contain approximately 60% diatoms, while the dark layers contain lower, but still significant, abundances of biogenic silica or biogenic carbonate. The biogenic content of the darker laminae is lower because they are either diluted by increased detrital supply or because biogenic supply was lower, perhaps from decreased productivity. In the oldest laminated zone, the laminae are thin (millimeter-scale) and well developed. These characteristics, together with the high organic carbon contents (Table 3) and absence of bioturbation in this interval, indicate that conditions at the sediment/water interface were unfavorable for benthic fauna at this time. In addition, laminae reflect repeated short-term variations in sediment supply. Such variations may occur annually or seasonally (Kemper and Zimmerle, 1980).

Repeated short-term (seasonal or annual?) variations in sediment supply are apparent in both the relative importances of biogenic and detrital components and the nature of the detrital constituents. Smear-slide analysis indicates that the lighter laminae contain only fine-grained (predominantly clay-sized) detrital material, in addition to the higher biogenic abundances described earlier. The darker laminae, however, contain a wider range of detrital grain sizes, including minor amounts of sand. Quantitative grain-size and compositional analyses of the terrigenous components in the light and dark laminae will be needed to determine sediment origin and mode of transport.

In lithologic Unit I overlying the laminated deposits of Unit II, the abundance of biogenic calcareous components increases upsection, while widespread bioturbation indicates a return to en-

vironmental conditions more favorable for benthic fauna. The transition to a biogenic calcareous sediment assemblage (vs. calcareous and siliceous) is completed by approximately 70 to 80 mbsf, with only marly calcareous nannofossil and foraminifer oozes occurring above that level. This transition is also evident in measurements of sediment density, organic carbon content, and carbonate content (Fig. 5 and Tables 3 and 7).

Although biogenic carbonate abundances increase upsection in Unit I, terrigenous abundances remain high. Inorganic calcite is a major detrital constituent, and its importance is at least partly responsible for the high carbonate abundances throughout lithologic Unit I. The origin of the inorganic calcite is not entirely clear, because it does not always co-vary with other phases that are demonstrably terrigenous (e.g., inorganic calcite increases, while quartz and clays decrease significantly). One explanation for this difference is that the sources and/or the transport processes of these phases are different. However, one possible source is reworking from shelly carbonate sands now forming on the shelf. Reworked foraminifers and aragonitic lenses derived from weathered shells were recognized while describing the Site 725 cores. When crushed, this material closely resembles the "inorganic calcite" observed in smear slides. Shore-based studies will investigate the sources of this calcite further by determining the relationship between calcite and palygorskite. Palygorskite is a known indicator of eolian supply from the Arabian Peninsula (Kolla et al., 1981, Caulet et al., in press), so that co-variation in inorganic calcite and palygorskite will support an eolian interpretation for the inorganic calcite.

In summary, lithologic Units I and III are compositionally similar in biogenic and terrigenous material. A major difference between the two units, however, is the higher organic carbon content of Unit III, which suggests that productivity and/or bottom-water conditions were different during the two periods of deposition. These differences may have developed because of changes in surface or deep-water circulation or they may have resulted from bathymetric changes produced by movement of Site 725.

The presence of upwelling flora in the laminated intervals and the increase in high organic carbon values (2%–3.5%) in

Table 3. Carbonate and organic carbon abundances at Site 725.

Hole, core, section, interval (cm)	Depth (mbsf)	Total carbon (%)	Inorganic carbon (%)	Organic carbon (%)	CaCO ₃ (%)
117-725C-1H-2, 90-92	2.40	6.95	6.45	0.50	53.7
725A-1H-3, 0-1	3.00	7.15	6.67	0.48	55.6
725C-1H-5, 90-92	6.90	7.17	6.42	0.75	53.5
725C-2H-2, 60-62	11.10	6.86	6.21	0.65	51.7
725C-2H-4, 60-62	14.10	7.08	6.03	1.05	50.2
725C-2H-7, 30-32	18.30	6.76	6.46	0.30	53.8
725C-3H-2, 100-102	21.10	6.32	5.86	0.46	48.8
725C-3H-4, 24-26	23.34	6.26	5.75	0.51	47.9
725C-3H-4, 119-120	24.29	6.83	6.49	0.34	54.1
725C-3H-6, 100-102	27.10	7.39	6.72	0.67	56.0
725C-4H-3, 50-52	32.00	7.00	6.58	0.42	54.8
725B-5X-2, 0-1	37.70	7.04	6.82	0.22	56.8
725C-6X-2, 86-88	49.86	7.46	6.43	1.03	53.6
725C-6X-2, 119-120	50.19	8.68	7.16	1.52	59.6
725C-6X-4, 86-88	52.86	7.11	6.23	0.88	51.9
725C-8X-3, 29-31	69.79	7.16	6.56	0.60	54.6
725C-9X-3, 119-120	80.29	6.93	6.18	0.75	51.5
725C-9X-4, 27-29	80.87	9.19	7.82	1.37	65.1
725C-11X-2, 24-26	97.04	7.84	5.50	2.34	45.8
725C-11X-5, 8-10	101.38	7.18	6.55	0.63	54.6
725C-12X-2, 19-21	106.59	12.32	8.73	3.59	72.7
725C-12X-3, 108-110	108.98	8.98	7.60	1.38	63.3
725C-12X-3, 119-120	109.09	7.79	6.94	0.85	57.8
725C-13X-3, 34-36	117.84	10.72	8.13	2.59	67.7
725C-14X-2, 21-23	125.81	11.68	8.33	3.35	69.4
725C-14X-4, 26-28	128.86	9.47	5.99	3.48	49.9
725C-14X-6, 14-16	131.74	7.91	4.48	3.43	37.3
725C-15X-2, 85-87	136.15	9.34	7.26	2.08	60.5
725C-15X-4, 80-82	139.10	7.41	4.25	3.16	35.4
725C-15X-4, 119-120	139.49	7.41	4.50	2.91	37.5
725C-16X-3, 4-6	146.54	10.54	6.63	3.91	55.2
725C-17X-2, 25-27	154.95	12.12	8.36	3.76	69.6
725C-17X-4, 106-108	158.76	6.87	3.25	3.62	27.1
725C-17X-5, 119-120	160.39	8.58	5.99	2.59	49.9
725C-17X-6, 128-130	161.98	9.12	4.96	4.16	41.3

lithologic Unit II indicate a major depositional change with respect to Units I and III, which supports the hypothesis that upwelling activity was different during the early Pleistocene than today. This may be interpreted in term of fluctuations in the strength of the monsoonal winds (Prell and Streeter, 1982). For that reason, shore-based research will consider both the productivity signal of the biogenic components and the source and transport record of the eolian components to describe sedimentation on the Oman margin in a more comprehensive manner.

BIOSTRATIGRAPHY

Introduction

Both planktonic and benthic foraminiferal fauna as well as nannofossils and radiolarians were studied at Site 725 to establish biostratigraphic zonations. Another objective was to investigate fluctuations in the upper boundary of the oxygen-minimum zone and possible changes in upwelling intensity.

The entire recovered section is referred to the Pleistocene. Planktonic and benthic foraminifera are abundant and well preserved throughout the section; nannofossils are abundant but are poorly preserved. Radiolarians are absent in the upper part of the sequence (Fig. 6). A plot of faunal datum levels vs. depth below the seafloor is presented in Figure 7; for a detailed list of these data points, see Table 4.

Planktonic Foraminifera

Planktonic foraminifera were studied in Hole 725C. The core-catcher samples contain highly diverse, well-preserved faunas throughout the entire sequence, except for Sample 117-725C-15X, CC (143.5 mbsf). This sample yields abundant, ro-

bust *Globorotalia tumida tumida* and common *Neoglobobulimina dutertrei* specimens, whereas thin-walled species are present only in low numbers. We believe this distribution of species is related to dissolution processes. The benthic foraminifera also are poorly preserved in this sample.

The presence of *Globigerinella calida calida* in Samples 117-725C-1H, CC through 117-725C-8X, CC (9.0-76.1 mbsf) marks Zone N23. *Globorotalia truncatulinoides* specimens are rare to common in the upper part of the section but disappear below Sample 117-725C-12X, CC (114.5 mbsf). However, some small specimens are again present in the lowermost sample (117-725C-17X, CC; 162.8 mbsf). Thus, the entire sequence is referred to the Pleistocene. The occurrence of *Globigerinoides fistulosus* in the same sample shows that the basal part of the Pleistocene was drilled, as the last appearance of this species has been dated at 1.6 Ma (Berggren et al., 1985).

Benthic Foraminifera

The benthic foraminiferal fauna was studied at Site 725 in the core-catcher samples of Hole 725C. Benthic foraminifera are abundant throughout the sequence, with a maximum abundance of about 140,000 specimens per 10 cm³ of sediment in Sample 117-725C-1H, CC (9.0 mbsf). Preservation is good to moderate but deteriorates downhole. Diversity is high, which can be expected in water this shallow (311 m).

The benthic foraminiferal fauna of Site 725 is relatively uniform and displays no significant changes during the short time interval recovered by the drilled sequence. However, one can recognize two slightly different assemblages. The first assemblage contains species that are abundant throughout the sequence: *Bolivina ordinaria*, *Cassidulina carinata*, *Cibicides wueller-*

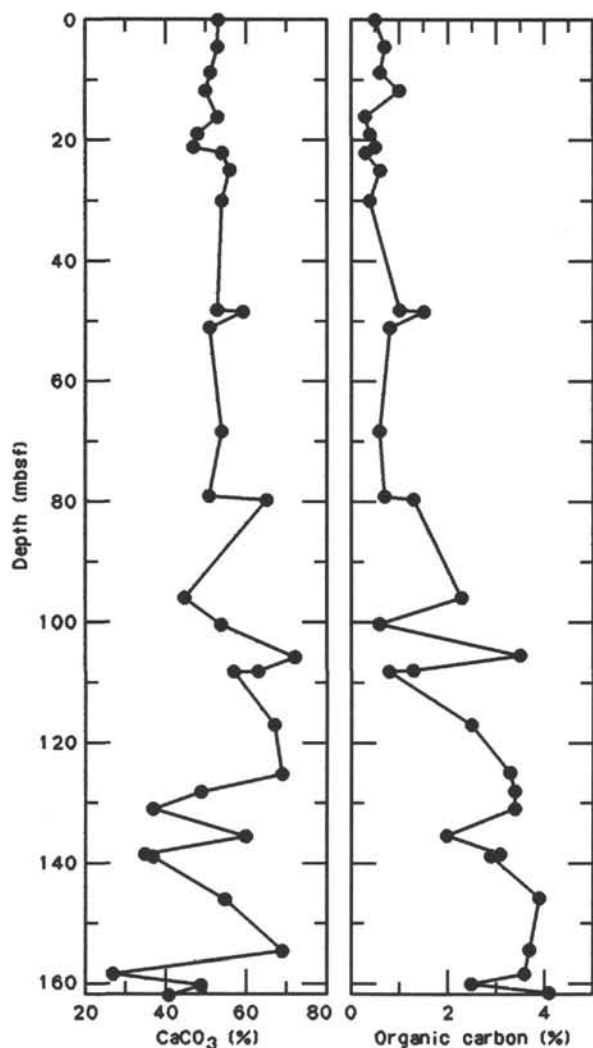


Figure 5. Carbonate and organic carbon profiles, Site 725.

Depth (mbsf)	Core	Epoch	Calcareous nannofossils	Radiolarians	Planktonic foraminifers	
	0	1	Pleistocene to Holocene	NN21	Barren	N23
2	2					
3	3					
4	4	NN20				
5	5					
6	6	NN19		Anthocyrtidium angulare		N22
7	7					
8	8					
9	9					
10	10					
11	11					
12	12					
13	13					
14	14					
15	15					
16	16					
17	17					

Figure 6. Correlation of planktonic microfossil zones in Hole 725C.

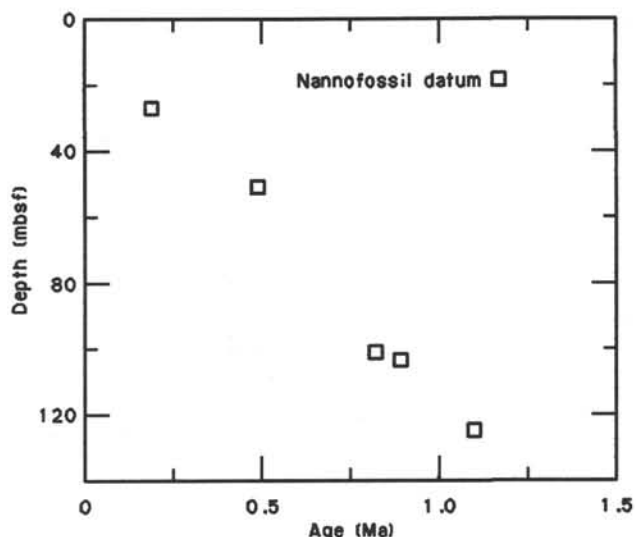


Figure 7. Age-depth plot for Hole 725C. For detailed list of events, see Table 4.

storfi, *Hyalinea balthica*, and *Uvigerina peregrina*. Additional species that occur only in this assemblage are *Ammonia beccarii*, *Lenticulina calcer*, and *Trifarina angulosa*. The other assemblage contains *Florilus* spp., *Globobulimina* spp., *Lenticulina* cf. *falcifer*, and *Uvigerina dirupta*, in addition to those species of the first assemblage. Assemblage 1 occurs in Sections 117-725-1H, CC through -9X, CC (9.0–85.7 mbsf), whereas the second assemblage occurs in Sample 117-725-10X, CC and down-hole to the bottom of the recovered sequence (95.3–162.8 mbsf).

The restriction of *Ammonia beccarii* to the upper 85 m may indicate a mid-Pleistocene uplifting at this site. The appearance of assemblage 2 coincides with an increase in the amount of phosphorite found and with a general decrease in the total number of specimens per volume.

Several large lenticuliids and nodosariids were found at Site 725; the diameter of the former often exceeds 5 mm.

Calcareous Nannofossils

Hole 725A

Because of drilling equipment failure, only one core was obtained from Hole 725A. The core-catcher material of this core (Sample 117-725A-1H, CC; 4.5 mbsf) contains *Emiliania huxleyi* and was assigned to Zone NN21 (upper Pleistocene to Holocene).

Holes 725B and 725C

At Hole 725B, penetration was 93.8 m; however, because of bottom-hole conditions, recovery of sediments was poor. The nannofossils recovered from this hole are abundant, but the assemblages are marked by low species diversity, which may be a result of comparatively low temperatures caused by upwelling. Preservation is generally poor. Sediments down to 17.2 mbsf contain *E. huxleyi* and belong to Zone NN21 (Holocene to upper Pleistocene). Below this zone, sediments down to 45.7 mbsf can be placed in Zone NN20 (Pleistocene) based on the absence of *E. huxleyi* and *Pseudoemiliania lacunosa*. The remaining sequence from 45.7 to 93.8 mbsf may belong to Zone NN19 (Pleistocene), although the abundances of *P. lacunosa* range from barren to common.

Nannofossil assemblages in Hole 725C are similar to those in Hole 725B (Fig. 8). Based on the same evidence as the previous hole, sediments down to 18.6 mbsf, underlying sediments down to 47.5 mbsf, and the remaining sediments down to 162.8 mbsf

Table 4. Stratigraphic list of faunal events for Hole 725C.

Event	Core level	Depth (mbsf)	Age (Ma)	Source of age	Notes
B <i>Emiliana huxleyi</i>	3H, 118-119	25.78	0.19	3	
T <i>Pseudoemiliana lacunosa</i>	6X-2, 118-119	50.18	0.49	3	
T <i>Reticulofenestra</i> sp. A	11X-3, 118-119	99.48	0.82	3	
B <i>Gephyrocapsa parallela</i>	11X-5, 93-94	102.23	^a 0.89	4	
T <i>Gephyrocapsa</i> "large" ^b	11X, CC	104.90			
T <i>Helicosphaera sellii</i>	13X, CC	124.10	^a 1.10	4	
	14X-1, 118-119	125.28			
	16X, CC	153.20			No good published age; event appears to be diachronous.
	17X-1, 129-130	154.49			

Note: T = upper limit of event and B = lower limit. Sources of ages are: 3 = oxygen isotope data for Site 723 (N. Niitsuma, unpubl. data); 4 = Takayama and Sato, 1987.

^a North Atlantic data

^b Long axis greater than 6 μ m.

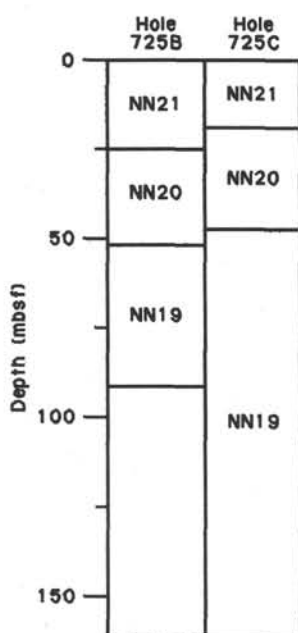


Figure 8. Correlation of calcareous nannofossil zones in Holes 725B and 725C.

were assigned to Zones NN21, NN20, and NN19, respectively. The nannofossil datums recognized in Hole 725C are tabulated in Table 4.

Additional Pleistocene calcareous nannofossil datums (see "Explanatory Notes" section, this volume, for explanation of datums) are recognized in Hole 725B as follows:

Datum 1	Uncertain
Datum 2	17.1-26.6 mbsf in Core 117-725B-3X
Datum 3	45.7-55.3 mbsf in Core 117-725B-6X
Datum 4	Uncertain
Datum 5	84.1-93.8 mbsf in Core 117-725B-10X
Datum 6	84.1-93.8 mbsf in Core 117-725B-10X

Rare reworked specimens were found in a few cores throughout Holes 725B and 725C. These include the Cretaceous species *Microrhabdulus decoratus* and *Discoaster multiradiatus* from the Paleocene or the Eocene.

Radiolarians

Sections 117-725B-1H, CC through 117-725B-10X, CC (7.5-93.8 mbsf) and 117-725C-11X, CC to 117-725C-17X, CC (104.9-

162.8 mbsf), which together form a continuous sequence, were examined for radiolarians. The upper 10 cores are barren. However, samples examined below that level have significant radiolarian fauna along with diatoms and sponge spicules. The presence of *Anthocyrtdium angulare* in Samples 117-725C-12X, CC (114.5 mbsf) and 117-725C-14X, CC (133.8 mbsf) places these samples, at least, in the *Anthocyrtdium angulare* Zone. The occurrence of *Lamprocyrtis neoheteroporos* in Samples 117-725C-16X, CC (153.2 mbsf) and 117-725C-17X, CC (162.8 mbsf) suggests that these samples probably lie within the *A. angulare* Zone as well. The fauna at this site is more diverse than at Site 724, although there are still few tropical zonal marker species.

Paleoenvironmental Implications

Many *Helicosphaera* specimens, which seem to prefer upwelling areas (Perch-Nielsen, 1985), as well as *Coccolithus pelagicus*, a cold-water species, were found in the lowermost core-catcher sample in Hole 725C (162.8 mbsf).

The presence of *Ammonia beccarii* in the upper part of the sequence indicates that this site has been at or above its modern water depth since approximately 0.7 Ma. The absence of the same species, together with a significantly different benthic foraminiferal fauna in the lower part of the sequence, might indicate a water depth exceeding 350 m before this date.

PALEOMAGNETISM

Introduction

Site 725 is located at 18°29.20' N, 57°42.03' E in water depth of about 310 m on the Oman margin. Holes 725A, 725B, and 725C were cored to depths of 4.5, 93.8, and 162.8 mbsf, respectively. The lithology consisted mainly of marly nannofossil ooze.

Magnetostratigraphy

As at Sites 723 and 724, natural remanent magnetization (NRM) intensities at Site 725 also were low, generally less than 1 mA/m (arithmetic mean = 0.7 mA/m) after alternating field (AF) demagnetization at 5 to 10 mT. Figure 9 depicts the combined discrete sample declination, inclination, and intensity data for Holes 725A, 725B, and 725C. Points having circular standard deviation values greater than 40° were excluded. Unfortunately, this (rather liberal) filtering procedure did not leave us enough points to permit detailed correlations with the polarity time scale. Reference to the nannofossil stratigraphy (see "Biostratigraphy" section, this chapter) suggests that the shallow and reversed inclination values at 79 mbsf may correspond to the Chron C1/C1r (Brunhes/Matuyama Chronozone) boundary, while the zone of normal inclinations at 100 and 121 mbsf

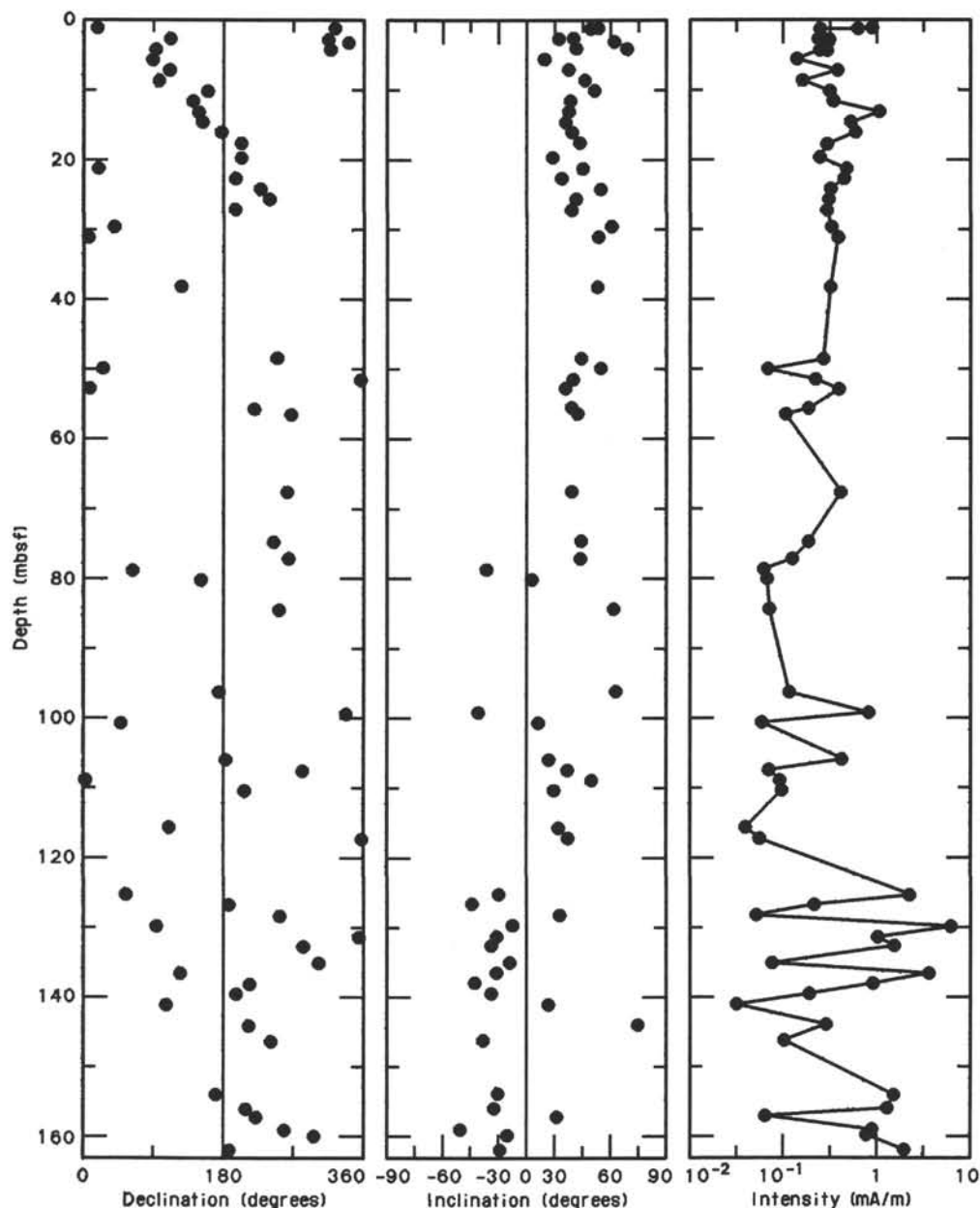


Figure 9. Declination, inclination, and intensity of discrete samples from Holes 725A, 725B, and 725C after AF demagnetization at 5–10 mT.

may be equivalent to Subchron C1r-1 (Jaramillo Subchron-zone). Shore-based study of samples collected (but not measured) on board the ship may enable us to make more confident correlations with the polarity time scale.

Figure 10 shows a histogram of inclination values (after filtering) grouped into 10° classes. Inclination values of the normally magnetized specimens agree with the expected geocentric axial dipole value for the site latitude (33.8°). Values for the reversely magnetized specimens appear significantly shallower than expected, which suggests the presence of a normal overprint that was not completely removed by AF demagnetization.

Magnetic Susceptibility

The volume magnetic susceptibility of Site 725 sediments was measured using the Bartington Instruments whole-core susceptibility sensor at the 0.1 sensitivity and low-frequency (0.47 kHz) settings. Intervals of 10 cm were measured at Hole 725C

only because of the poor recovery in Holes 725A and 725B. Gas expansion was most severe in Cores 117-725C-16X and -17X; thus, to avoid gaps, archive halves were measured and data were multiplied by two during processing. Susceptibility data for Hole 725C are shown in Figure 11. Poor recovery below Core 117-725C-4H (~ 32 mbsf) limited the usefulness of the susceptibility data for intersite correlations. Some correlations with Sites 723 and 724 are possible for the first four cores of Hole 725C, however.

While the gaseous nature of Hole 725C sediment precluded measuring susceptibility continuously, the self-extrusion of Hole 725C sediments during core-splitting provided copious amounts of material that could not be curated, which we found suitable for magnetic extractions. Approximately 0.25 kg of wet sediment obtained from the top of Section 117-725C-5H-1 (~ 38 mbsf) was dispersed in ~ 1 L of Calgon solution. The slurry was continuously agitated while two bar magnets (sheathed in para-

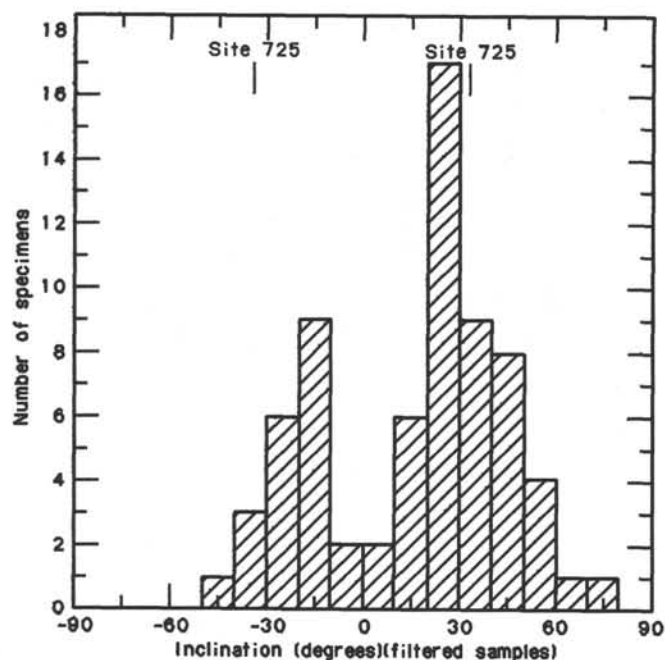


Figure 10. Inclination values grouped into 10° classes. Arrows indicate the expected geocentric axial dipole value for the site latitude.

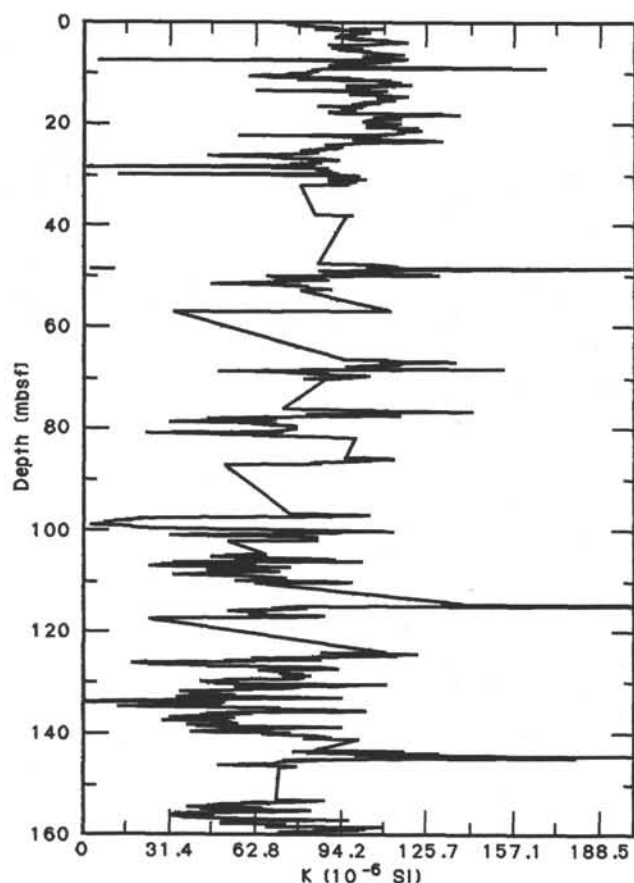


Figure 11. Whole-core magnetic susceptibility record for Hole 725C.

film) were positioned at the top and bottom levels of the beaker. The magnets were removed after several minutes, and the adhering magnetic residue was washed into a separate beaker each time. This process was repeated approximately 15 times for each

of two aliquots of sediment. This extraction procedure was then applied to the primary extracts for purification. The efficiency of the extraction is unknown. Visual inspection indicated that the extracted grains were quite coarse (medium silt), which suggests that the finer grains contributing to the NRM either were not abundant or were not extracted.

The initiative for extracting magnetic particles came from our desire to observe the grain sizes, shapes, and textures that contributed to susceptibility and remanence. The slight down-hole decrease in NRM intensity from 0 to ~100 mbsf (Fig. 9) suggests that fine-grained ferrimagnetic particles may be dissolving or altering to nonmagnetic phases. The final purified extraction was divided into highly magnetic and less magnetic fractions by passing a bar magnet under the beaker containing the purified extraction and drawing the most magnetic particles to one side. These grains were removed by pipette, dried, and mounted on an SEM sample stub for observation at high magnification. Photographs of the observed grains are shown in Figures 12 through 14.

Observation of the grains indicated that they were remarkably uniform in size (fine to coarse silt) and were generally well rounded and well preserved. Uniformity of size may have been a consequence of the extraction procedure. The degree of grain roundness was surprising in that an extract from margin sediment might be expected to be more angular. However, the roundness is consistent with an eolian mode of deposition, as suggested by the XRD data presented in the "Paleomagnetism" section of the Site 722 chapter.

Some indication of grain pitting and dissolution can be seen in many of the photographs. Striking examples of this can be seen in Figure 13 and in the upper right quadrant of Figure 14. Extensive pitting was apparent for about 10% of the grains, while moderate pitting included perhaps another 10%. Generally, however, the preservation of the grains was very good. To better understand the history of magnetic mineral deposition, we intend to conduct more thorough shore-based magnetic and morphometric analyses of magnetic extracts from Leg 117 sediments.

ACCUMULATION RATES

Sedimentation rates for the top 100 m (lithologic Unit I) of Site 725 are calculated between nannofossil datums with ages based on oxygen isotope stratigraphy (Table 4; Niitsuma, unpublished data). The mean rate for the last million years ranges from 79 to 152 m/m.y. (Table 5, Fig. 15), with an overall average of 124 m/m.y. If we include two additional nannofossil datums recognized at Site 725, with ages based on North Atlantic data (Table 4), the mean rate is 114 m/m.y. for the last 1.1 m.y. (Fig. 15). These values are typical of hemipelagic sedimentation in the upper slope basin. No reliable stratigraphic markers were found below 125 mbsf, therefore, sedimentation rate are unavailable for lithologic Units II and III.

The mass accumulation of calcium carbonate, organic carbon, and noncarbonate sediment components were calculated from average values between nannofossil datums (Table 6, Fig. 16). Based on the homogeneous sediment character in lithologic Unit I, this large variation in accumulation rate is unexpected and may be attributed to uncertainties in the age model. Post-cruise studies that obtain a more precise age model for Site 725 will be necessary to verify these rate changes.

PHYSICAL PROPERTIES

Introduction

Physical properties measured on discrete samples of sediment recovered from Site 725 included only index properties (wet-bulk density, porosity, water content, and grain density). The sediments recovered were not sufficiently indurated to allow

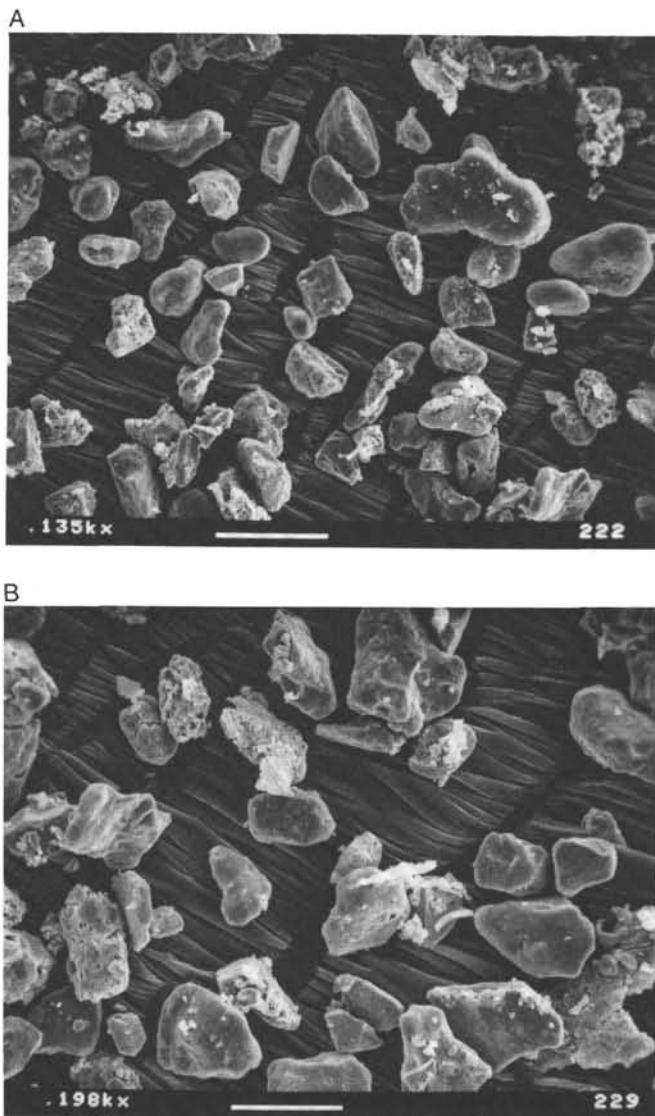


Figure 12. Scanning electron microscope photograph of magnetic concentrates from Site 725 sediments.

compressional-wave velocities to be measured with the Hamilton Frame Velocimeter. The coarse-grained noncohesive sediments common in the upper part of this site were not suitable for measuring shear strengths with the Wykeham-Farrance vane shear device. The properties that were determined for discrete samples from Holes 725A and 725B, and Hole 725C are listed in Tables 6 and 7, respectively. Wet-bulk density was measured on all whole-round core sections that were at least 80 cm long using the GRAPE logging system. Acquisition of compressional-wave velocity data using the *P*-wave logger was successful only on the cores recovered using the APC coring system. All techniques and equipment used are described in the "Explanatory Notes" (this volume).

Index Properties

Lithologic Unit I

Lithologic Unit I (0–121.0 mbsf) is made up of several sediment types that, on the basis of visual description, were not divided into facies or subunits. However, index properties of the sediments in lithologic Unit I do show two distinct trends (Fig. 17) that are related to minor changes in sediment composition

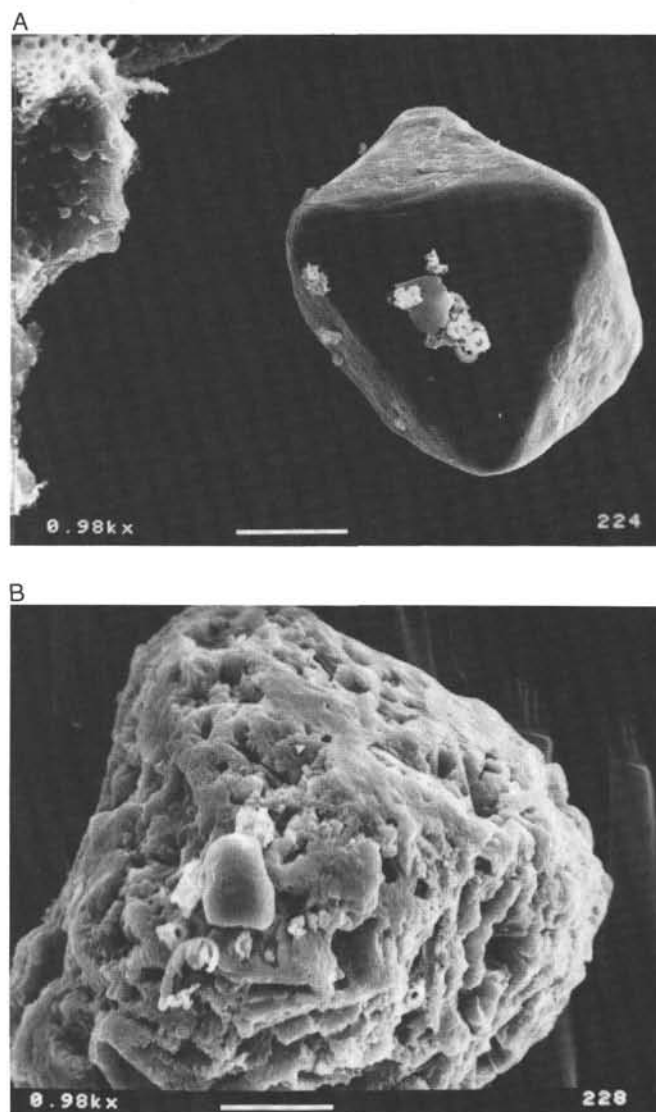


Figure 13. Scanning electron microscope photograph of magnetic concentrates from Site 725 sediments.

and a decrease in grain size downsection. From the seafloor to 70 mbsf, lithologic Unit I is a coarse-grained unit that consists primarily of foraminifer-rich, calcitic, sandy silt and calcitic, marly, nannofossil ooze, throughout which the percentages of calcium carbonate (average of 53%) and organic carbon (< 1%) are nearly constant with depth (see "Lithostratigraphy" section, this chapter, Fig. 15). At 70 mbsf, average values of porosity and water content decrease gradually with depth from 51% to 49% and 30% to 28%, respectively. Wet-bulk density reflects the downsection decrease in water content, which increases from 1.87 g/cm³ near the seafloor to 1.93 g/cm³ at 70 mbsf. Variations in the values of porosity, water content, and wet-bulk density may be partly attributed to local variation in sediment composition and fabric, but may also be a result of the inevitable disturbance during core recovery of unconsolidated sands and silts. The low porosity and density gradients determined here are typical of coarse-grained sediments, which decrease volume slowly during the early stages of compaction (Meade, 1966). Because of the strong possibility of disturbance, however, the porosities, water contents, and bulk densities reported here should be considered as lower and upper bounds, respectively, on the *in-situ* values.

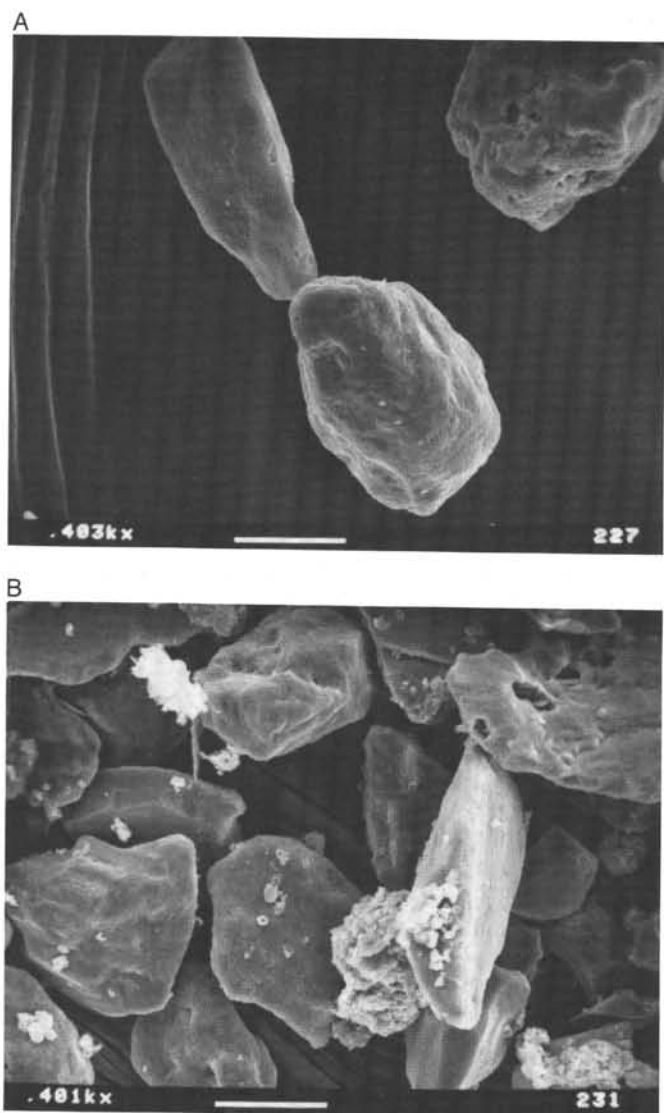


Figure 14. Scanning electron microscope photograph of magnetic concentrates from Site 725 sediments.

In the lower part of lithologic Unit I (75–121 mbsf), the physical property trends change in response to the increasing abundance of terrigenous clay, as well as to gradual increases in both calcium carbonate and organic carbon throughout the section (see “Lithostratigraphy” section, Fig. 15). Although no distinct sedimentologic boundary was identified, physical properties change abruptly near the top of Core 117-725C-9X (76 mbsf), where porosity and water content increase to 66% and 42%, respectively. Between 76 and 121 mbsf, porosity and water content decrease gradually and uniformly to 64% and 40%, respectively. One deviation from this trend occurs in a sample taken from a calcitic silty clay, Sample 117-725C-12X-3, 108–110 cm, which shows inexplicably low porosity and water content coupled with high wet-bulk density. Grain density generally decreases from 2.60 to 2.55 g/cm³ over this interval in which diatoms become increasingly abundant with depth and nannofossils replace a portion of the terrigenous material (see “Lithostratigraphy” section, this chapter; Fig. 17). Wet-bulk density shows considerable variation over this interval (1.62–1.83 g/cm³) and averages 1.68 g/cm³.

Lithologic Unit II

Within the laminated layers of calcitic marly nannofossil ooze and diatomaceous clayey silt and mud of lithologic Unit II (121.0–145.4 mbsf) porosity, water content, and wet-bulk density are relatively constant, with the exception of one sample taken from one of the diatomaceous layers in Sample 117-725C-14X-6, 14–16 cm. The highest porosity (71%) and water content (50%) measured at Site 725 were measured in this diatomaceous interval. Porosity and water content average 63% and 39%, respectively, for the entire unit. Wet-bulk density averages 1.66 g/cm³ through lithologic Unit II as a whole and decreases to 1.44 g/cm³ within the diatomaceous mud. Grain densities continue to decrease downsection, with a minimum value of 2.31 g/cm³ in the diatom-rich layer of Core 117-725C-14X.

Lithologic Unit III

Within lithologic Unit III (145.4–162.8 mbsf), index properties resume the downsection trends established in the base of lithologically similar Unit I. Porosity and water content at the base of this unit average 59% and 37%, respectively. Wet-bulk densities and grain densities measure 1.66 and 2.59 g/cm³, respectively.

GRAPE and P-Wave Logs

Data collected by the GRAPE logging system were of good quality in Hole 725C, in part because of the relatively low gas content of the section (Figs. 18 and 19). The major gaps in the records correspond to intervals of no recovery, rather than areas of low data quality. The general pattern of density variation displayed on the GRAPE records follows that of the wet-bulk densities determined for discrete samples. In the uppermost 70 m of Hole 725C, GRAPE records show relatively high density (1.9 g/cm³) that varies less than 0.2 g/cm³. As with the discrete samples, density decreases and variability of the values increases abruptly near 80 mbsf. A close correspondence between the GRAPE logs and discrete samples continues downsection to lithologic Unit III, where the quality of the GRAPE data degrades as the diameter of the core decreases, producing a gap between the sediment and core liner.

Good quality *P*-wave logs were obtained in Cores 117-725C-1H through -4H. The high, near-surface values, 1600 to 1700 m/s, reflect the low densities of the coarse-grained sediment. The *P*-wave record for Cores 117-725C-5X through -11X is of poor quality because of spotty recovery, but does reflect the decrease in density displayed in the GRAPE records. At depths below 100 mbsf, incomplete filling of the core liners resulted in a lack of coupling between sediment and liner that prevented the transmission of *P*-wave signals.

Patterns of cyclic variation on a scale of several meters displayed on the records from Sites 721, 722, 723, and 724 are not well defined at Site 725 because of the low variability in both density and velocity in the surficial sediments.

INORGANIC GEOCHEMISTRY

Introduction

Eight interstitial water samples were collected at Site 725 by squeezing: one each from Holes 724A and 724B and the remainder from Hole 724C. No *in-situ* samples were collected from this site. All analytical results are listed in Tables 8 and 9 and presented in Figures 20 and 21. These profiles are compiled from data from all three holes.

Salinity, Chloride, and pH

The concentration profiles of salinity, chloride, and pH are shown in Figure 20. There is a loss of salinity with depth (~2 g/

Table 5. Sedimentation and accumulation rate data for Site 725.

Depth interval (mbsf)	Age range (m.y.)	CaCO ₃ (̄%)	C _{org} (̄%)	Dry-bulk density (̄g/cm ³)	Sed. rate (̄m/m.y.)	CaCO ₃ acc. rate (g/cm ² /k.y.)	Non-CaCO ₃ acc. rate (g/cm ² /k.y.)	C _{org} acc. rate (mg/cm ² /k.y.)
0-27.1	0-0.19	52.5	0.57	1.41	142.6	10.56	9.55	114.6
27.1-50.9	0.19-0.49	55.8	0.32	1.54	79.3	6.81	5.40	39.1
50.9-100.9	0.49-0.82	54.6	1.21	1.19	151.5	9.84	8.18	218.1

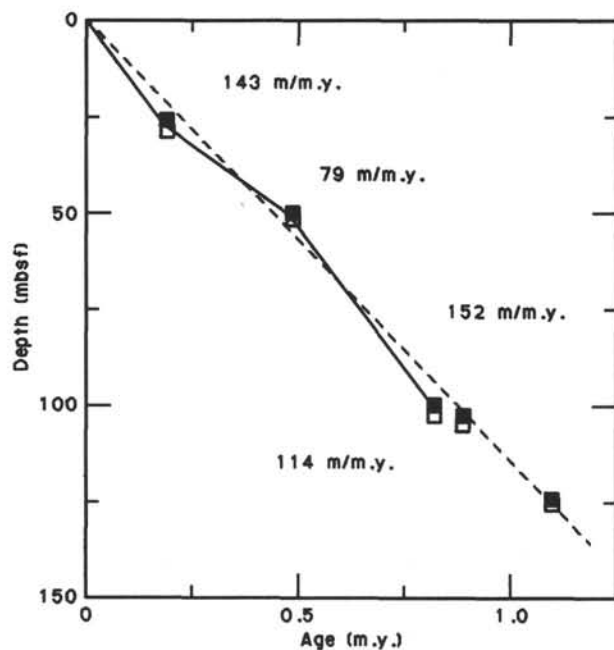


Figure 15. Age-depth plot of stratigraphic datums listed in Table 4. The filled and open boxes are the upper and lower depths of each datum level, respectively. Indicated sedimentation rates (solid lines) are calculated between reliable nannofossil datum levels. The dashed line represents the mean sedimentation rate for the last 1.1 m.y. at Site 725, based on a best fit to all stratigraphic data.

kg over 160 m) of the same magnitude as occurs at Site 724. This decrease may also be attributed to depletion of sulfate and magnesium ions that are involved in microbial degradation and diagenetic reactions, respectively.

The chloride profile at Site 725 displays similar structure to that seen at Site 724, where a broad maximum was observed between 20 and 100 mbsf. However, at Site 725 the chloride maximum extends over a greater depth zone and reaches higher concentrations (+14 mmol/L relative to the topmost sample, compared to a ~10 mmol/L increase at Site 724). We believe that this chloride maximum may represent burial of late Pleistocene seawater that was more saline than modern bottom water. Subsequent diffusion is gradually smoothing this signal. It is not clear why the chloride maximum is seen only at Sites 724 and 725.

pH values measured at this site are biased by sample degassing. However, Site 725 has a slightly higher pH than Site 724, although this may result from the lower depressurization of these samples (Site 725 was one-half as deep as Site 724).

Sulfate and Alkalinity

Sulfate depletion occurs over the upper 110 m of the cored section (Fig. 20), giving a gradient of ~-0.25 mmol/L/m.

This is one-half the gradient of Site 724, despite the higher rate of sedimentation at this site (see "Biostratigraphy" section, this chapter). Below ~110 mbsf, sulfate is constant at ~1 mmol/L, similar to the distribution seen at Site 724.

In contrast to sulfate, the alkalinity increase observed at this site is more than three times that at Site 724. Approximately 30 mmol/L of titration alkalinity was observed at the point where the sulfate concentration approaches zero, compared with ~10 mmol/L at the previous site. Although an alkalinity deficit (about 20 mmol/L) still occurs at this site, the absolute difference between the profiles at the base of the sulfate reduction zones at the two sites may be attributed to less carbonate precipitation in the rapidly accumulating sandy terrigenous sediment of Site 725. Faster sedimentation would cause concentration gradients for alkalinity, magnesium, and calcium to become less steep, which in turn would reduce the downward flux of the alkaline earths, and thus alkalinity, to reaction sites at depth. The increase in alkalinity below 110 mbsf is probably from ammonia production during methanogenesis (see below).

Calcium and Magnesium

Both calcium and magnesium concentrations (Fig. 20) decrease with depth, although calcium displays a subsurface maximum at ~50 mbsf. The profiles indicate that little reaction is occurring in these sediments, while diffusion plays a major role in determining the gradients observed (especially for magnesium). The low magnesium/calcium ratio, low alkalinity deficit, and high accumulation rate of the sediment conspire to limit dolomite diagenesis in the upper 150 m of this site.

Ammonia, Phosphate, Silica, and Dissolved Organic Carbon (DOC)

The distribution of these constituents is shown in Figure 20. Ammonia concentrations increase down the length of the cored section, with a gradient (~0.13 mmol/L/m) similar to that observed at Site 724.

Phosphate concentrations are low and variable (perhaps due to analytical difficulties). The low values are most likely caused by the phosphatization of biogenic skeletal debris and/or apatite precipitation on calcite tests.

Dissolved silica increases rapidly at 40 to 50 mbsf from ~300 μ mol/L to ~1200 μ mol/L, which is near the saturation limit of opal-CT at this water depth. This rapid increase suggests that biogenic silica should be observed in the sediment in greater amounts from 50 mbsf. In a similar fashion, DOC (Table 9 and Fig. 20) increases over the same depth zone, suggesting that greater amounts of biogenic matter occur within the sediment column below 50 mbsf. Total organic carbon (see "Organic Geochemistry" section, this chapter) and sediment smear-slide descriptions (see "Lithostratigraphy" section, this chapter) indicate relatively constant organic matter concentrations of ~1.0 wt% over the top 80 m of Site 725, but increasing (to 3.5 wt%) and variable concentrations of organic matter and diatoms below. The interstitial water geochemistry presented here broadly confirms these observations.

Table 6. Physical properties summary for Holes 725A and 725B.

Core, section, interval (cm)	Depth (mbsf)	Wet-bulk density (g/cm ³)	Porosity (%)	Water content (%)	Grain density (g/cm ³)	Dry-bulk density (g/cm ³)
117-725A-1H-1, 100-102	1.00	1.883	49.4	26.9	2.615	1.376
725A-1H-3, 100-102	4.00	1.844	51.9	28.8	2.642	1.312
725B-5X-1, 100-102	37.20	1.970	46.9	24.4	2.681	1.490
725B-6X, CC 15-17	46.49	2.039	40.4	20.3	2.608	1.625
725B-7X-1, 130-132	56.60				2.643	

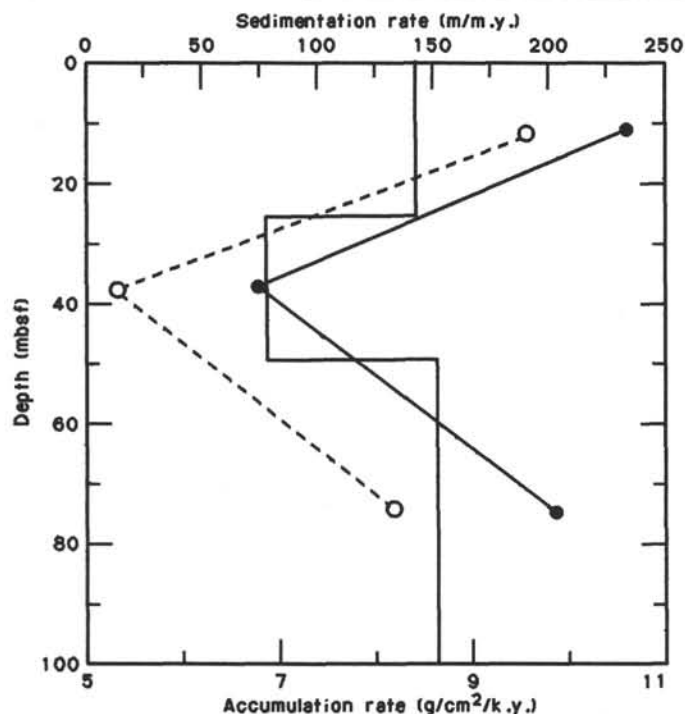


Figure 16. Sedimentation rate (m/m.y.; solid line), calcium carbonate accumulation rate (g/cm²/k.y.; filled circles), and noncarbonate accumulation rate (g/cm²/k.y.; open circles) vs. depth (mbsf) at Site 725. Accumulation rates are plotted at the midpoint of the respective depth intervals.

ORGANIC GEOCHEMISTRY

Abundance and Character of Organic Matter

The headspace residues as well as the physical properties residues of 35 samples (mainly from Hole 725C) were analyzed for their calcium carbonate and organic carbon content; the results are given in Table 3 and plotted vs. depth in Figure 5. Organic carbon and calcium carbonate values are fairly constant in the upper 80 mbsf of lithologic Unit I, and organic carbon averages only 0.65%, a low value when compared to previous sites drilled on the Oman margin. The entire lithologic Unit I down to 120 mbsf (see "Lithostratigraphy" section, this chapter), which consists of foraminifer-rich, calcitic, calcareous ooze and sandy silt, has an average value of 1.0%. Organic carbon concentrations vary widely in the lower 40 m of Unit I and reach high values of 3.6%, which are characteristic for the underlying unit of laminated and diatomaceous sediments that comprise lithologic Unit II (120.0-145.4 mbsf). We believe that the facies and composition of Unit II indicate suboxic deposition during some part of the lower Pleistocene. Average organic carbon concentrations are 3.06%. Below Unit II, sediments have the same aspect as those in lithologic Unit I and consist of nanofossil-rich calcitic sand, silt, and clay that averages 3.61% organic carbon. Sparse pyrolysis results (Table 10) indicate that samples from lithologic

Unit I with low organic carbon values have low hydrogen index (HI) values, an indication of relatively refractory organic matter. Two samples from Units II and III show high values that appear to be related to the higher organic carbon content. Currently, we are not certain whether influx determines the relative freshness of the organic matter, or whether preservational signals prevail (Fig. 21).

Hydrocarbon Gases

Because of the very shallow water depth (311 m), safety considerations made a stringent hydrocarbon monitoring program necessary at Site 725. Gas pockets occurred only in the last four cores of Hole 725C; results of analyses of the vacutainer samples are given in Table 11. Methane is the most abundant gas, but considerable amounts of thermogenic ethane and propane were detected in gas pockets of Core 117-725C-17X (Table 11). Headspace samples were taken at regular intervals in Hole 725C; results appear in Table 12. Again, a steady increase of the thermogenic gases, ethane and propane, was observed with depth.

SUMMARY AND CONCLUSIONS

Site 725 marks a shallow landward end point of a depth transect designed to recover sediments from a water depth range of 300 to 1500 m on the Oman continental margin. This transect brackets the vertical extent of a pronounced mid-water oxygen-minimum zone. Site 725 is located on the landward flank of the prominent slope basin that had been drilled at Sites 723 and 724. The goal for Site 725 was to trace the fluctuations in the upper boundary of the oxygen-minimum zone through time and to evaluate these fluctuations with regard to changes in the monsoonal upwelling, eolian transport, and eustatic sea level. Continuity of the sedimentary section and the benthic foraminifer assemblages were expected to reveal any differential tectonic movement of the basement blocks and the slope basins.

Some of the major findings at Site 725 are summarized in Figure 22 and include the following:

1. Identification of the alternation of millimeter-scale laminated organic- and opal-rich clayey silt with nonlaminated nanofossil ooze and calcitic silty clay. The laminated intervals are confined to a brief interval in the lower Pleistocene.
2. The average sedimentation rate is about 120 m/m.y.
3. Opal occurrences are confined to sediments with high organic carbon concentrations and overlap the laminated intervals.
4. Cold-water nannoplankton occurrences at the base of the section and abundant but low-diversity assemblages throughout the overlying section.
5. Persistent occurrence of interstitial sulfate, high alkalinities, and dramatic core expansion, which indicate replenishment of the interstitial sulfate pool at depth, comparable to Site 723.
6. A maximum in the chloride concentration at about 80 mbsf (~0.7 Ma), which was also seen at Site 724, suggests that mid-Pleistocene bottom water on the upper margin was significantly more saline than it is today.

Table 7. Physical properties summary for Hole 725C.

Core, section, interval (cm)	Depth (mbsf)	Wet-bulk density (g/cm ³)	Porosity (%)	Water content (%)	Grain density (g/cm ³)	Dry-bulk density (g/cm ³)
117-725C-1H-2, 90-92	2.40	1.915	50.8	27.2	2.724	1.395
1H-6, 90-92	8.40	1.842	53.6	29.8	2.749	1.293
2H-2, 60-62	11.10	1.953	45.7	24.0	2.635	1.484
2H-4, 60-62	14.10	1.815	51.7	29.2	2.647	1.286
2H-7, 30-32	18.30	1.924	46.2	24.6	2.665	1.450
3H-2, 100-102	21.10	1.956	47.5	24.9	2.673	1.469
3H-4, 24-26	23.34	1.956	47.6	24.9	2.639	1.468
3H-6, 100-102	27.10	1.936	46.8	24.8	2.656	1.457
4X-3, 50-52	32.00	1.998	45.0	23.1	2.714	1.537
6X-2, 86-88	49.86	1.810	52.7	29.8	2.677	1.271
6X-4, 86-88	52.86	1.840	51.9	28.9	2.617	1.308
8X-3, 29-31	69.79	1.935	47.2	25.0	2.664	1.452
9X-4, 27-29	80.87	1.622	66.5	42.0	2.592	0.941
11X-2, 24-26	97.04	1.622	64.7	40.9	2.556	0.959
11X-5, 8-10	101.38	1.838	52.5	29.3	2.631	1.300
12X-2, 19-21	106.59	1.586	66.8	43.2	2.513	0.901
12X-3, 108-110	108.98	1.802	66.6	37.8	2.633	1.120
13X-3, 34-36	117.84	1.631	63.0	39.6	2.524	0.985
14X-2, 21-23	125.81	1.623	65.5	41.3	2.621	0.952
14X-4, 26-28	128.86	1.670	61.1	37.5	2.513	1.044
14X-6, 14-16	131.74	1.444	71.0	50.4	2.309	0.716
15X-2, 85-87	136.15	1.737	59.9	35.3	2.662	1.123
15X-4, 80-82	139.10	1.604	64.6	41.3	2.484	0.942
16X-3, 4-6	146.54	1.673	60.2	36.9	2.476	1.056
17X-2, 25-27	154.95	1.653	59.4	36.8	2.436	1.044
17X-4, 106-108	158.76	1.664	58.2	35.9	2.499	1.068
17X-6, 128-130	161.98	1.663	60.8	37.4	2.506	1.040

7. Elevated ethane and propane gas concentrations with depth imply migration of thermogenic hydrocarbons from deep sources.

The section penetrated at Site 725 ranges from the Holocene to the lower Pleistocene and has been subdivided into three lithologic units (Fig. 22).

Lithologic Unit I (0-120 mbsf) comprises foraminifer-rich, calcitic, sandy silt to calcitic, marly, calcareous ooze; calcitic, marly, nannofossil ooze; and nannofossil-rich sand, silt, or clay. This lithology is coarser and has more detrital carbonate than similar sediments at Sites 723 and 724. It is considered to be a hemipelagic facies dominated by influx of detrital calcite, eolian silts and clays, and biogenic components from coastal upwelling and modified by slight winnowing or nondeposition of fine-grained material. Organic carbon content is less than 1% over the upper 80 m and varies between 1% and 2% in the lower part of the unit.

Lithologic Unit II (120-145.4 mbsf) is composed of diatomaceous clayey silt and diatomaceous mud intercalated with calcitic marly nannofossil ooze and calcitic sand, silt, and clay (Fig. 25). Diatom-rich beds form laminae on less than a centimeter scale and are dominated by frustules of two diatom species. The unit is believed to indicate anoxic depositional conditions. Organic carbon content ranges between 2% and 3% in this laminated unit.

Lithologic Unit III (145-162.8 mbsf) is similar to Unit I and is composed of nannofossil-rich, calcitic sand, silt, and clay and calcitic, marly, nannofossil ooze. All units were found to contain less than 2% authigenic dolomite and traces of apatite and fish scales. Organic carbon content averages 3%.

Like previous sites on the margin, Site 725 contains partially overlapping intervals of cold-water nannoplankton species and a robust, radiolarian fauna dominated by Spumellarians (Fig. 22). In contrast to the other sites, these occurrences are confined to the lower Pleistocene. However, the opal-rich sediments coincide with the laminated facies, as observed at other sites.

Mass accumulation rates obtained with a preliminary age model are depicted in Figure 22. These rates may vary by almost a factor of two downhole. However, some of this variation may be attributed to uncertainties in the age and depth of biostratigraphic datums.

Comparison of Site 725 with Site 723 demonstrates that the ratio of organic matter accumulation to clastic and biogenic accumulation is higher at Site 723 in the center of the basin than at Site 725. This pattern of accumulation may indicate a persistent spatial inhomogeneity of primary production and preservation, or an influx of allochthonous organic-carbon-rich material.

Even though dolomite was encountered in trace amounts throughout the cores, the extent of dolomitization was insignificant when compared to the pronounced dolomitization observed at Site 723. Interstitial water profiles at Site 725 show an increase in chloride concentrations with depth. Sulfate ions are never depleted at depth, even though increasing ammonia and alkalinity concentrations imply ongoing sulfate reduction at depth (Fig. 22). Thus, a replenishment of the interstitial sulfate pool by ascending water may be implied. The persistence of sulfate reduction is in accord with relatively low methane concentrations in gas pockets. Cores more than 100 mbsf show increasing (up to 90 $\mu\text{L/L}$) ethane and propane concentrations that are believed to indicate thermal hydrocarbon generation at depth.

Site 725 constitutes a complete section of Pleistocene age that shows significant changes in the oceanographic and depositional environment, such as the frequency of upwelling indicators, the accumulation of carbon, and the preservation of laminated facies. Similar associations were observed at Sites 723 and 724, and these associations seem roughly contemporaneous. If these facies prove to be synchronous, they will provide constraints on the regional vs. local origin and possible extent of the oxygen-minimum zone. A preliminary interpretation of the heterogeneity observed in organic matter abundance and preservation of primary sediment structures (i.e., the laminations) is

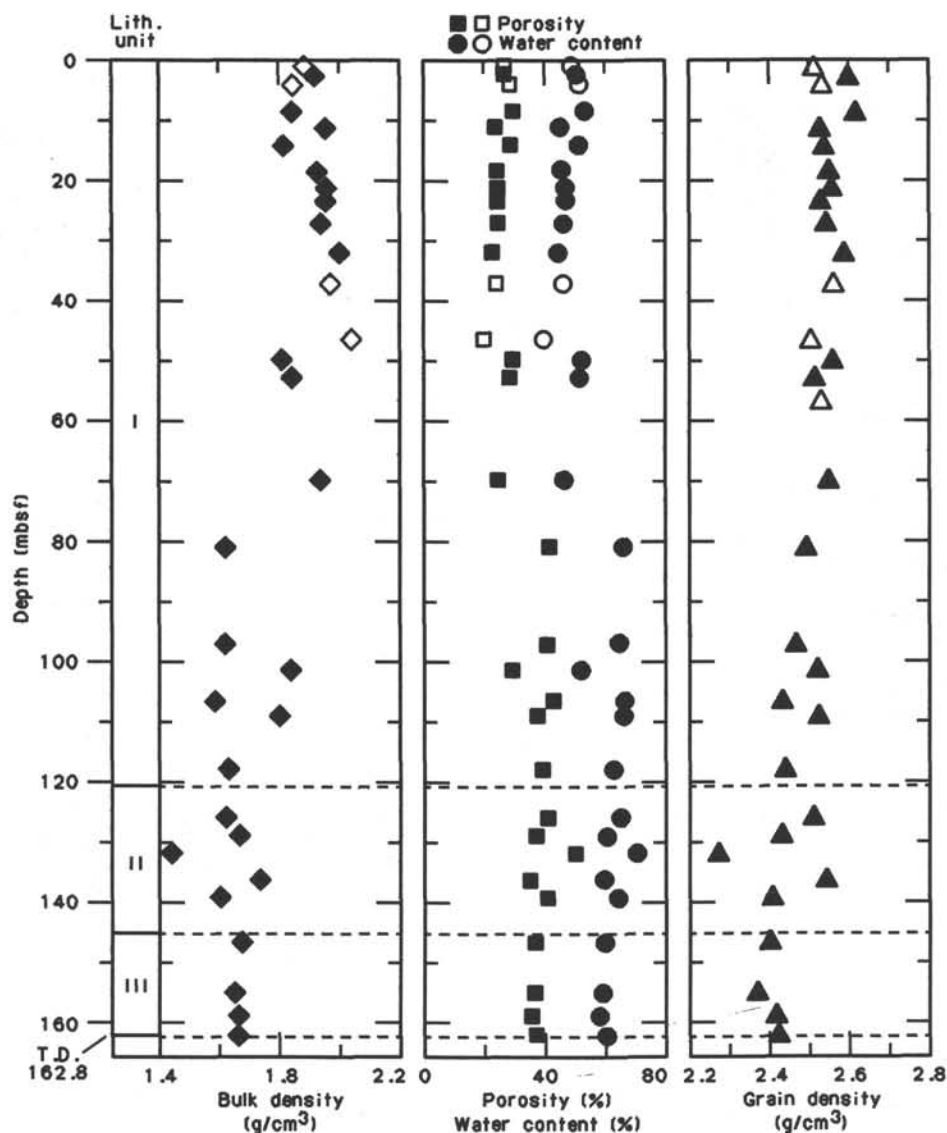


Figure 17. Index properties (bulk density, porosity, water content, and grain density) measured on discrete samples from Holes 725A, 725B, and 725C. Hole 725A and 725B = open symbols; Hole 725C = closed symbols.

that the mid-water oxygen-minimum zone expanded, perhaps in response to enhanced productivity, and was more stable during the early Pleistocene.

REFERENCES

- Berggren, W. A., Kent, D. V., and Van Couvering, J. A., 1985. The Neogene: Part 2, Neogene geochronology and chronostratigraphy. In Snelling, N. J. (Ed.), *The Chronology of the Geological Record*. Geol. Soc. Mem. (London), 10:211-260.
- Caulet, J. P., Debrabant, P., and Fieux, M., in press. Dynamique des masses d'eau océanique et sédimentation quaternaire sur la marge de l'Afrique de l'Est et dans le bassin de Somalie. Résultats préliminaires de la mission MD44 INDUSOM du Marion-Dufresnes. *CRAS*.
- Emerson, S., 1985. Organic carbon preservation in marine sediments. In Sundquist, E. T., and Broecker, W. S. (Eds.), *The Carbon Cycle and Atmospheric CO₂: Natural Variations Archean to Present*. Geophys. Monogr., 3:78-87.
- Kemper, E., and Zimmerle, W., 1980. Facies pattern of a Cretaceous/Tertiary subtropical upwelling system (Great Syrian Desert) and an Aptian/Albian boreal upwelling system (NW Germany). In Thiede, J., and Suess, E. (Eds.), *Coastal Upwelling* (Pt. B): New York (Plenum Press), 29-72.
- Kolla, V., Kostecki, J. A., Robinson, F., and Biscaye, P. E., 1981. Distributions and origins of clay minerals and quartz in surface sediments of the Arabian Sea. *J. Sediment. Petrol.*, 51:563-569.
- Meade, R. H., 1966. Factors influencing the early stages of compaction of clays and sands—review. *J. Sediment. Petrol.*, 36:149-165.
- Perch-Nielsen, K., 1985. Cenozoic calcareous nannofossils. In Bolli, H., Saunders, J., and Perch-Nielsen, K. (Eds.), *Plankton Stratigraphy*: Cambridge (Cambridge Univ. Press), 427-554.
- Prell, W. L., and Streeter, H. F., 1982. Temporal and spatial patterns of monsoonal upwelling along Arabia: a modern analogue for the interpretation of Quaternary SST anomalies. *J. Mar. Res.*, 40:143-155.
- Takayama, T., and Sato, T., 1987. Coccolith biostratigraphy of the North Atlantic Ocean, Deep Sea Drilling Project Leg 94. In Ruddiman, W. F., Kidd, R. B., Thomas, E., et al., *Init. Repts. DSDP, 94*, Pt. 2: Washington (U.S. Govt. Printing Office), 651-702.

Ms 117A-112

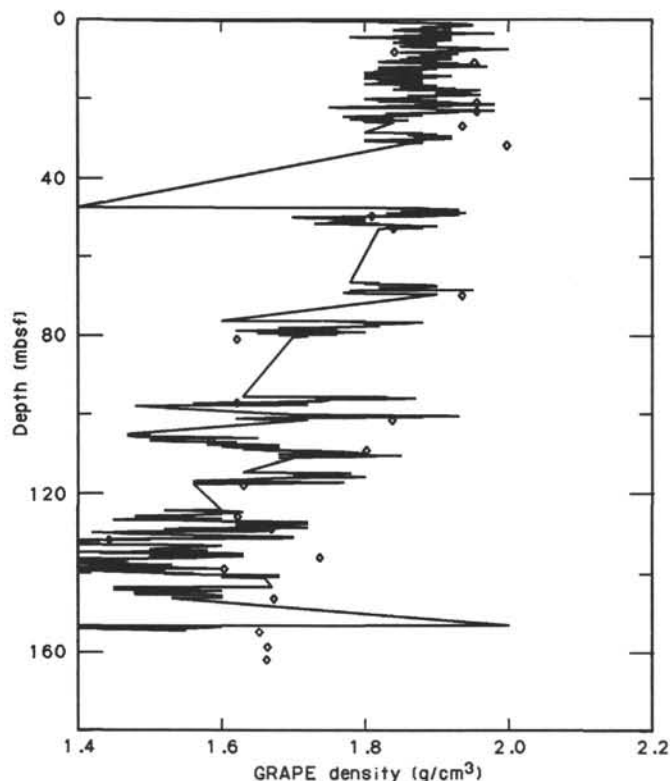


Figure 18. GRAPE wet-bulk density (solid line) and wet-bulk density from discrete samples (diamonds) for Hole 725C. GRAPE profile is based on 10-cm-block averages of the data.

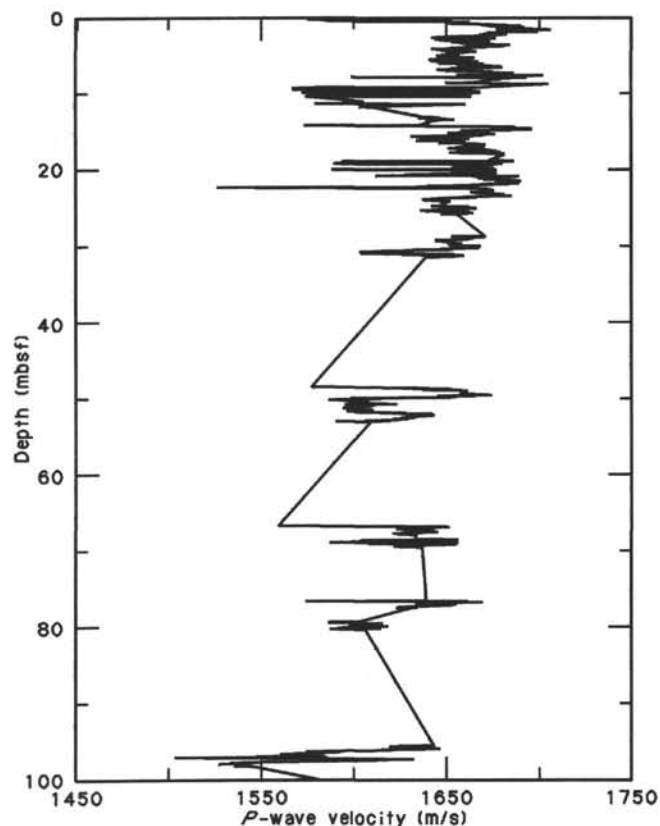


Figure 19. Compressional-wave velocity as measured by the *P*-wave logger in Cores 117-725C-1H through Section 117-725C-11X-2.

Table 8. Summary of interstitial-water geochemical data at Site 725.

Core, section, interval (cm)	Depth (mbsf)	Vol. (mL)	pH	Alk. (mmol/L)	Sal. (g/kg)	Mg (mmol/L)	Ca (mmol/L)	Cl (mmol/L)	SO ₄ (mmol/L)	PO ₄ (μmol/L)	NH ₄ (mmol/L)	SiO ₂ (μmol/L)	Mg/Ca (μmol/L)
117-725A-1H-2, 145-150	2.95	30	7.70	3.67	35.6	54.32	10.63	576	27.2	2.8	0.65	183	5.11
725B-5X-1, 145-150	37.65	30	8.15	4.77	35.6	46.11	13.03	583	21.3	1.6	1.40	310	3.54
725C-3H-4, 145-150	24.55	42	8.37	4.66	35.5	46.95	11.96	584	21.5	1.2	1.02	248	3.93
725C-6X-2, 145-150	50.45	39	8.29	10.56	35.4	43.60	12.00	587	15.5	6.4	3.10	914	3.63
725C-9X-3, 145-150	80.55	40	8.05	17.31	36.0	41.90	13.49	592	13.5	3.6	4.53	1272	3.11
725C-12X-3, 145-150	109.35	43	7.96	27.16	34.8	31.12	8.75	583	0.8	5.1	9.15	1195	3.56
725C-15X-4, 145-150	139.75	45	8.32	32.20	34.2	27.41	7.34	569	1.1	2.0	16.47	1262	3.73
725C-17X-5, 145-150	160.65	38	7.95	33.93	34.2	22.13	5.39	565	0.8	2.0	21.34	1135	4.11

Table 9. Dissolved organic carbon concentrations at Site 725.

Core, section, interval (cm)	Depth (mbsf)	Dissolved organic carbon (a.u.)
117-725A-1H-2, 145-150	2.95	0.097
725C-3H-4, 145-150	37.65	0.455
725B-5X-1, 145-150	24.55	0.625
725C-6X-2, 145-150	50.45	1.085
725C-9X-3, 145-150	80.55	0.891
725C-12C-3, 145-150	109.35	1.187
725C-15X-4, 145-150	139.75	1.031
725C-17X-5, 145-150	160.65	0.995

Note: a.u. = absorbance units.

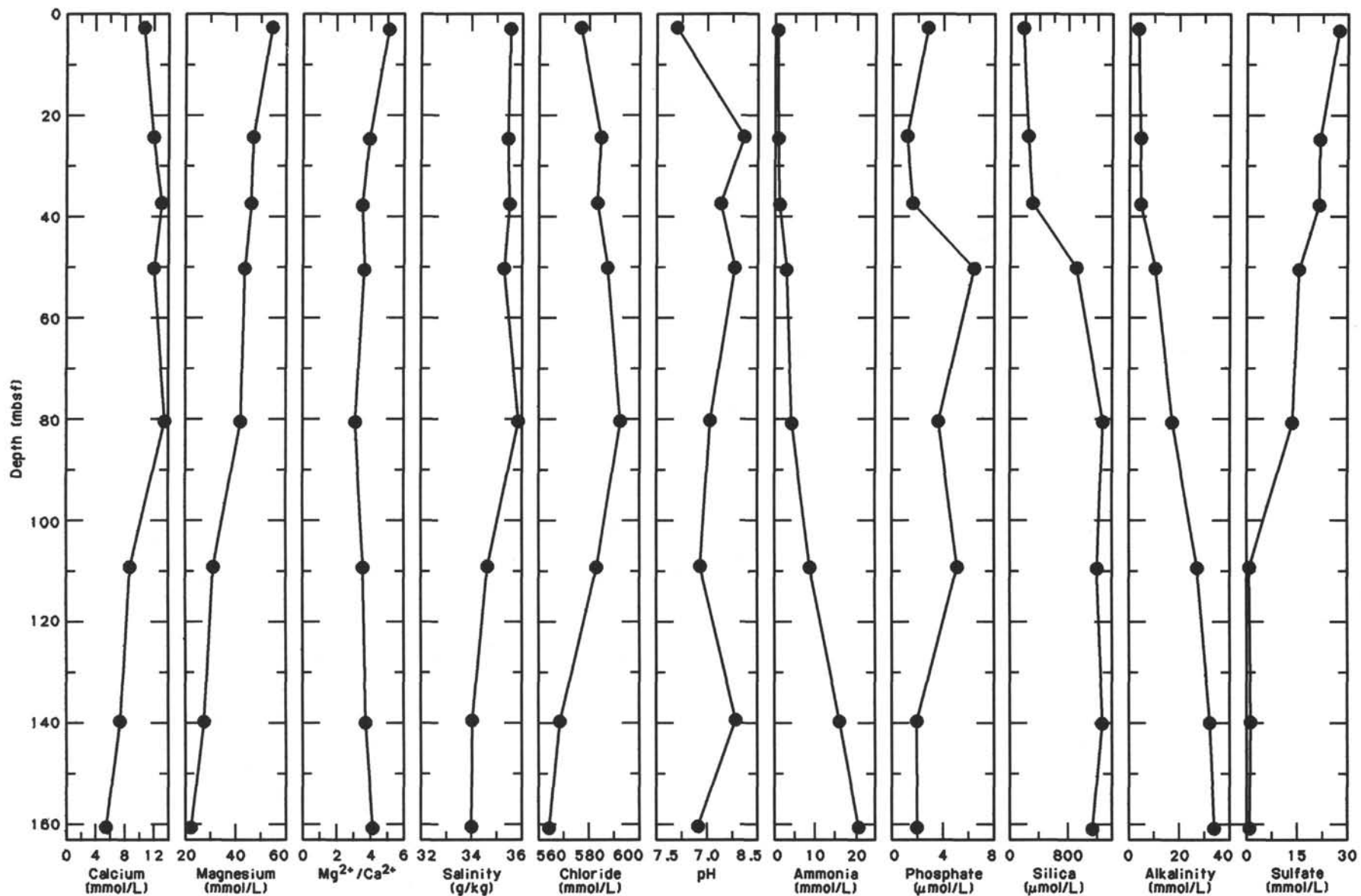


Figure 20. Profiles of interstitial water concentrations for Site 725, compiled from data from three holes.

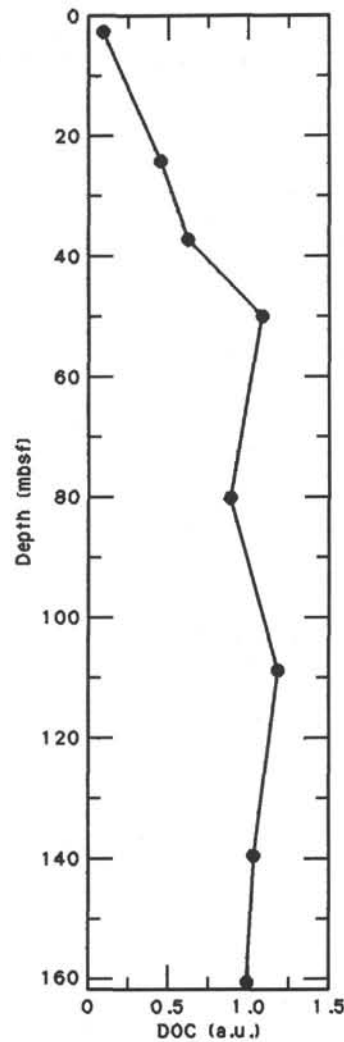


Figure 21. Dissolved organic carbon (DOC) profile for Site 725, compiled from data from three holes (expressed as absorbance units).

Table 10. Results of Rock-Eval pyrolysis of headspace residues from Holes 725A, 725B, and 725C.

Core, section, interval (cm)	Depth (mbsf)	T _{max} (°C)	S ₁	S ₂	S ₃	S ₂ /S ₃	TOC ^a	TOC ^b	HI	OI
117-725A-1H-1, 0-3	3.00	413	0.17	0.70	1.46	0.47	0.45	0.48	146	304
725C-3H-4, 119-120	24.29	412	0.04	0.25	1.04	0.24	0.18	0.34	73	305
725C-6X-2, 119-120	50.19	416	0.31	2.02	1.50	1.34	0.82	1.52	133	99
725C-9X-3, 119-120	80.39	418	0.31	1.49	1.16	1.28	0.45	0.75	199	155
725C-12X-3, 119-120	109.09	415	0.45	1.89	1.25	1.51	0.50	0.85	222	147
725C-15X-4, 119-120	139.49	403	3.61	10.37	2.58	4.01	2.64	2.91	356	89
725C-17X-5, 119-120	160.39	400	2.18	8.64	2.54	3.40	2.21	2.59	333	98

Note: HI = hydrogen index and OI = oxygen index; the hydrogen and oxygen indexes were calculated on the basis of the TOC^b values. For a detailed description of parameters, see "Explanatory Notes," chapter (this volume).

^a TOC values are measured by Rock-Eval pyrolysis.

^b TOC values measured by difference method.

Table 11. Concentrations of methane (C₁), ethane (C₂), and propane (C₃) measured in gas pockets from Hole 725C.

Core, section, interval (cm)	Depth (mbsf)	C ₁ (ppm)	C ₂ (ppm)	C ₃ (ppm)	C ₁ /C ₂
117-725C-14X-6, 28	131.88	412,173	134	19	3,076
15X-3, 14	136.94	255,992	74	11	3,459
16X-1, 145	144.95	142,217	30	5	4,741
17X-6, 30	161.00	799,315	295	52	2,709

Table 12. Concentrations of methane (C₁), ethane (C₂), and propane (C₃) per liter of wet sediment in samples from Holes 725A, 725B, and 725C.

Core, section, interval (cm)	Depth (mbsf)	C ₁ (μL/L)	C ₂ (μL/L)	C ₃ (μL/L)	C ₁ /C ₂
117-725A-1H-3, 0-1	3.00	342			
725B-5X-2, 0-1	37.70	11			
725C-3H-4, 119-120	24.29	38			
725C-6X-2, 119-120	50.19	95	2		48
725C-9X-3, 119-120	80.29	304	6		51
725C-12X-3, 119-120	109.09	52,023	18	3	2,890
725C-15X-4, 119-120	139.49	54,575	29	22	1,882
725C-17X-5, 119-120	160.39	62,010	48	38	1,292

Note: Values are expressed in μm (volume gas/volume wet sediment).

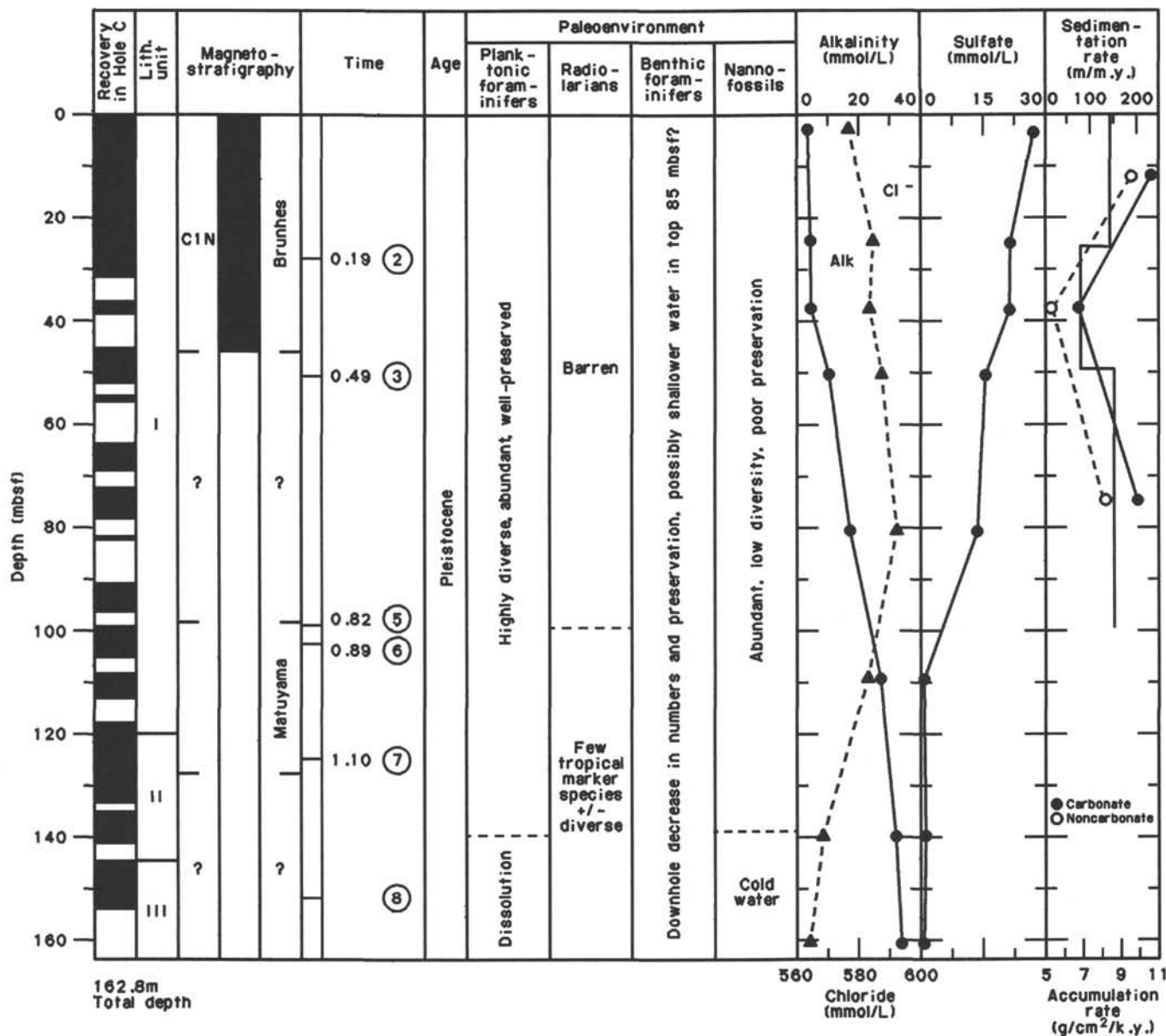


Figure 22. Summary chart outlining preliminary shipboard findings at Site 725. Numbers in circles: nannofossil marker horizons.